CHEMISTRY
A European Journal

A Journal of
ChemPubSoc Europe

Accepted Article

Title: Highly electron rich β-diketiminato systems: Synthesis and coordination chemistry of amino functionalized 'N-nacnac' ligands

Authors: Dinh Cao Huan Do, Ailsa Keyser, Andrey Protchenko, Brant Maitland, Indrek Pernik, Haoyu Niu, Eugene Kolychev, Arnab Rit, Dragoslav Vidovic, Andreas Stasch, Cameron Jones, and Simon Aldridge

To be cited as: *Chem. Eur. J.* 10.1002/chem.201700757

Link to VoR: http://dx.doi.org/10.1002/chem.201700757

Supported by
ACES

WILEY-VCH

10.1002/chem.201700757

WILEY-VCH

Highly electron rich β-diketiminato systems: Synthesis and coordination chemistry of amino functionalized 'N-nacnac' ligands

Dinh Cao Huan Do,[a] Ailsa Keyser,[a] Andrey V. Protchenko,[a] Brant Maitland,[b] Indrek Pernik,[b] Haoyu Niu,[a] Eugene L. Kolychev,[a] Arnab Rit,[a] Dragoslav Vidovic,[c] Andreas Stasch,*[b,d] Cameron Jones,*[b] and Simon Aldridge*[a]

Abstract: The synthesis of a class of electron-rich amino-functionalized β-diketiminato (N-nacnac) ligands is reported, with two synthetic methodologies having been developed for systems bearing backbone NMe_2 or NEt_2 groups and a range of N-bound aryl substituents. In contrast to their (Nacnac)H counterparts, the structures of the protio-ligands feature the bis(imine) tautomer and a backbone CH_2 group. Direct metallation with lithium, magnesium or aluminium alkyls allows access to the respective metal complexes via deprotonation of the methylene function; in each case X-ray structures are consistent with a delocalized imino-amide ligand description. Trans-metallation using lithium N-nacnac complexes has then been exploited to access *p* and *f*-block metal complexes which allow for like-for-like benchmarking of the N-nacnac ligand family against their more familiar Nacnac counterparts. In the case of Sn^{II} the degree of electronic perturbation effected by introduction of the backbone NR_2 groups appears to be constrained by the inability of the amino group to achieve effective conjugation with the N_2C_3 heterocycle. More obvious divergence from established structural norms are observed for complexes of the larger, harder Yb^{II} ion, with azaallyl/imino and even azaallyl/NMe_2 coordination modes being demonstrated by X-ray crystallography.

Introduction

The mono-anionic β-diketiminate (or 'Nacnac') ligand class, $[R''C(R'CRN)_2]^-$, has been widely employed in the stabilization of metal complexes from across the Periodic Table.[1,2] In part, this reflects the strongly electron-donating properties of these systems, allied to their potential for forming thermodynamically stable complexes through chelation, and the ready tuning of their steric properties through the N-alkyl/aryl substituents. As such, a number of recent landmark compounds from the *s*-, *p*-, *d* and *f*-blocks have drawn on Nacnac supporting frameworks.[3,4]

While tuning the steric demands of the N-substituents to modulate access to the metal centre is relatively easily accomplished, variation in ligand electronic properties has been examined to a lesser extent.[4c] The incorporation of electronically modifying substituents within the N-aryl groups, for example, has been examined, although the extent of communication with the N-donor itself is presumably dependent on the torsional alignment of the aryl ring.; another option is to modify the nature of the backbone C-bound groups, with examples including trifluoromethyl, and electron-withdrawing aryl substituents having been reported.[5] Bearing in mind the differences in the donor capabilities of amidinato and guanidinato ligands derived from the inclusion of a pendant NR_2 group,[6] we hypothesized that the incorporation of a similar backbone π-donor into a Nacnac ligand framework might lead to enhanced donor properties (Scheme 1). In Valence Bond terms the electronic perturbation brought about by the inclusion of peripheral NR_2 substituents can be viewed as resulting from additional 'double amido' resonance structures incorporating a pendant $=NR_2^+$ function.

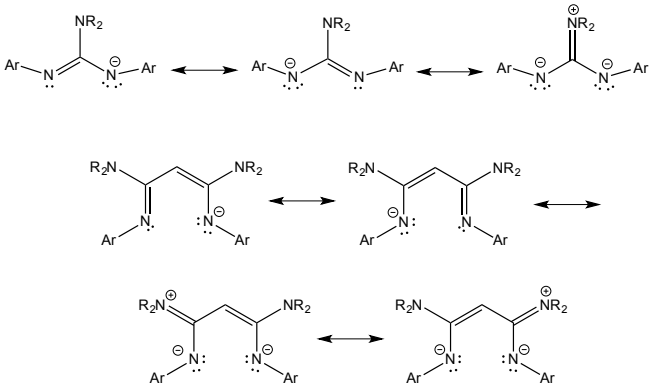

Scheme 1. Potential resonance forms for (upper) guanidinato and (lower) amino-functionalized Nacnac ligands.

While unpublished theoretical studies appear to corroborate this viewpoint,[7] and synthetic studies giving access to protio-ligands employing an $-NMe_2$ substituent date back to 1971,[7,8]

[a] Mr D Do, Dr A Protchenko, Ms A Keyser, Mr H Niu, Dr E Kolychev, Dr A Rit, Prof S Aldridge
Department of Chemistry, University of Oxford, Inorganic Chemistry Laboratory, South Parks Road, Oxford, UK. OX1 3QR
E-mail: Simon.Aldridge@chem.ox.ac.uk
[b] Dr B Maitland, Dr I Pernik, Dr A Stasch, Prof C Jones
School of Chemistry, Monash University, PO Box 23, Melbourne, Victoria 3800, Australia
E-mail: Cameron.Jones@monash.edu
[c] Dr D Vidovic
SPMS-CBC, Nanyang Technological University, 21 Nanyang Link, Singapore, 637371.
[d] *Present address: EaStCHEM School of Chemistry, University of St Andrews, North Haugh, St Andrews, KY16 9ST, United Kingdom. E-mail: as411@st-andrews.ac.uk*

Supporting information for this article is given via a link at the end of the document.

10.1002/chem.201700757

little attempt has been made to systematically appraise the chemistry of amino-functionalized Nacnac (or N-nacnac) ligands.[9] With this in mind, we set out to explore the synthetic, coordination and structural chemistry of this ligand family, and to compare their properties with those of the corresponding (backbone Me) Nacnac systems.

Results and Discussion

Protio-ligand synthesis and structural characterization. Two different approaches have been investigated for the synthesis of the target (N-nacnac)H protio-ligands, involving either (i) the condensation of RNH_2 (R = aryl, alkyl) with a pre-formed bifunctional backbone or (ii) the coupling of two amino-imine units though the C2 backbone position (Scheme 2).

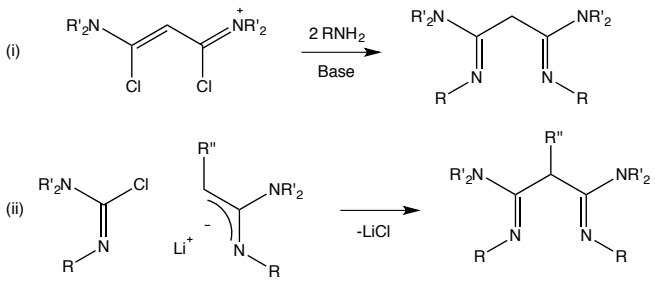

Scheme 2. The two different synthetic routes to (N-nacnac)H protio-ligands investigated in the current study.

Route (i) was optimized based on a procedure originally reported by Viehe *et al.* in 1971, and subsequently explored by Clyburne.[7,8] This approach involves initial reaction between Viehe's Salt (dichloromethylene-dimethyliminium chloride) and *N*,*N*-dimethyl-acetamide, followed by *in situ* addition of the aniline of choice to yield the protio-ligands, [**1**^{R}]H (Scheme 3). The two aryl groups initially chosen [R = Ph and Dipp (2,6-$^{i}Pr_2C_6H_3$)], were designed to probe the scope for variation in steric bulk compatible with this synthetic approach.

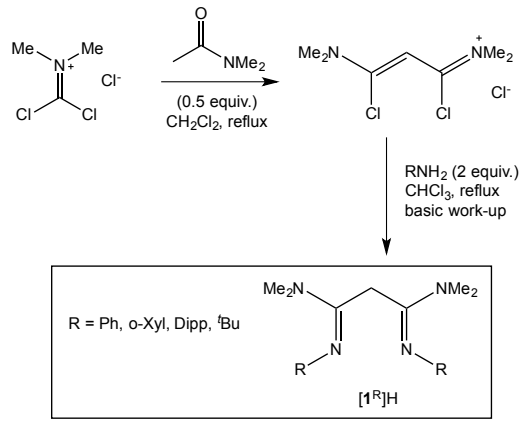

Scheme 3. Condensation based synthetic route to (N-nacnac)H protio-ligands of the type [**1**^{R}]H.

The resulting protio-ligands [**1**^{Ph}]H and [**1**^{Dipp}]H can be obtained as analytically pure materials (in yields of 50-60 and 30-40%, respectively) either directly without further purification (in the case of [**1**^{Ph}]H) or following recrystallization from acetone/hexane (for [**1**^{Dipp}]H). Both NMR studies in hydrocarbon solution and crystallographic studies in the solid state reveal differences in the structures of [**1**^{Ph}]H/[**1**^{Dipp}]H compared to the corresponding (Nacnac)H protio-ligands. In the (Nacnac)H systems hydrogen-bonding between the N-H proton and the imine N atom helps to stabilize a planar conjugated amino-imine tautomer.[10] By contrast, in the (N-nacnac)H systems [**1**^{Ph}]H and [**1**^{Dipp}]H, intramolecular hydrogen bonding is absent and the diimine structure pertains, allowing for much longer distances between the two imine N atoms and relief of steric congestion caused by the pendant aryl groups (Figure 1).

The lack of conjugation about the NCCCN unit in [**1**^{Ph}]H/[**1**^{Dipp}]H is consistent with C1-C2 and C2-C3 distances determined crystallographically which are in the C-C single bond range (e.g. 1.527(2) Å and 1.524(1) Å, respectively, for [**1**^{Ph}]H).[11] Consistently, the imine C-N distances (e.g. 1.292(1) Å and 1.288(1) Å for [**1**^{Ph}]H), are typical of isolated C-N double bonds [11] On the other hand, the corresponding exocyclic C1-N3 and C3-N4 distances (e.g. 1.360(2) Å and 1.374(1) Å for [**1**^{Ph}]H) are found to lie between C-N single and double bond ranges, indicating a degree of conjugation of the lone pairs of the NMe_2 units into the imine functions.

^{1}H NMR spectroscopy provides evidence that the diimine form of [**1**^{Ph}]H/[**1**^{Dipp}]H is also retained in solution, showing in each case a signal integrating to two protons for the saturated methylene linker (at δ_H = 3.37 and 3.27 ppm for [**1**^{Ph}]H/[**1**^{Dipp}]H,

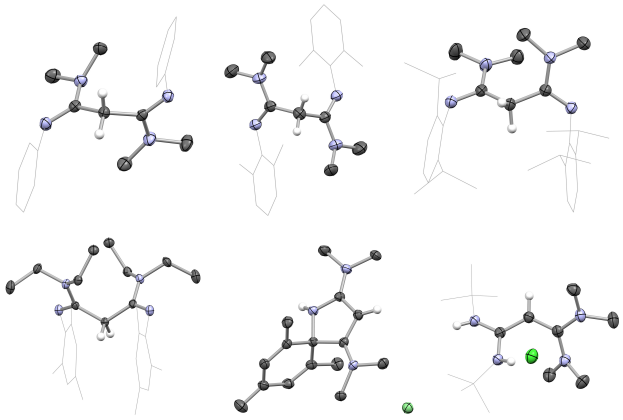

Figure 1. Molecular structures (upper) of [**1**^{Ph}]H, [**1**^{Xyl}]H and [**1**^{Dipp}]H, and (lower) of [**4**^{Mes}]H, **2** and **3** in the solid state as determined by X–ray crystallography. Colour scheme: hydrogen, white; carbon, grey; nitrogen, pale blue; chlorine, green. Displacement ellipsoids drawn at 50 % probability level; most H-atoms and solvate molecules omitted, and N-substituents drawn in wireframe format for clarity. Key bond lengths (Å) and angles (°): (for **2**): C16-C20 1.351(4), C15-C16 1.454(3), C13-C15 1.336(3), C12-C13 1.529(3), C12-C18 1.520(3), C17-C18 1.334(3), C16-C17 1.459(3); (for **3**): C8-C14 1.411(2), C14-C15 1.407(2), C8-N7 1.348(2), C8-N9 1.353(2), C15-N16 1.366(2), C15-N19 1.348(2). Key metrical data for [**1**^{Ph}]H, [**1**^{Xyl}]H, [**1**^{Dipp}]H and [**4**^{Mes}]H are given in Table 1.

Table 1. Crystallographically determined bond lengths (Å) for (N-nacnac)H protio-ligands.

Protio-ligand	*d*(C1-N1),[a] *d*(C3-N2)	*d*(C1-N3), *d*(C3-N4)	*d*(C1-C2), *d*(C2-C3)
[**1**^{Ph}]H	1.292(1) 1.288(1)	1.360(2) 1.374(1)	1.527(2) 1.524(2)
[**1**^{Xyl}]H	1.283(3)	1.369(3)	1.526(3)
[**1**^{Dipp}]H	1.287(2) 1.286(2)	1.365(2) 1.367(2)	1.512(2) 1.529(2)
[**4**^{Mes}]H	1.292(2)	1.371(2)	1.529(2)

[a] See Figure 2 for atom numbering scheme. [b] Metric parameters given for one of the molecules in the asymmetric unit.

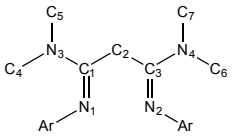

Figure 2. Atom numbering scheme used in Table 1 for compounds [**1**^{Ph}]H, [**1**^{Xyl}]H, [**1**^{Dipp}]H and [**4**^{Mes}]H.

respectively) and no resonances in the regions expected for an N-H proton or for the γ-CH unit of an amino-imino system (cf. δ_H = 12.12 ppm and 4.84 ppm, respectively, for {HC(MeCDippN)$_2$}H in $CDCl_3$).[12]

DFT calculations carried out for [**1**^{Ph}]H and [**1**^{Dipp}]H at the BP86-D3(TZP) level reveal that the energetic difference between the diimine and amino-imine forms is small ($|\Delta E| < 10$ kJ mol^{-1}) both in the gas phase and in simulated benzene or chloroform solution (Table 2 and Figure 3). While these calculations indicate that the diimine tautomer is marginally favored for [**1**^{Ph}]H, and that the energy difference is essentially zero for [**1**^{Dipp}]H, the analogous calculations for the related (Nacnac)H compounds (with backbone methyl substituents) indicate a slightly larger energetic preference (ΔE > 25 kJ mol^{-1}) in the opposite sense, *i.e.* favoring the amino-imine form. Presumably such differences reflect, at least in part, a greater increase in delocalization achieved for X = Me on adoption of the amino-imine tautomeric form (Figure 3), *i.e.* a greater gain in

Table 2. DFT calculated energies of diimine and amino-imine tautomers for (N-nacnac)H and (Nacnac)H protio-ligands .

Ligand	X	R	Δ*E* (kJ mol^{-1})[a]		
			Gas-phase	Benzene	Chloroform
(N-nacnac)H	NMe_2	Ph	-6.5	-8.3	-9.0
	NMe_2	Dipp	+0.6	+0.8	+0.8
(Nacnac)H	Me	Ph	+35.3	+28.7	+25.6
	Me	Dipp	+60.0	+36.1	+35.6

[a] Δ*E* = *E*(dimine form) – *E*(amino-imine form). A negative figure therefore indicates that the diimine tautomer possesses a lower overall energy.

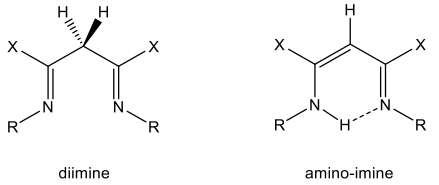

Figure 3. Potential diimine and amino-imine tautomers for (N-nacnac)H and (Nacnac)H protio-ligands.

conjugation associated with linking two isolated imine units over the corresponding process for two amidine functions.

Interestingly, the one-pot synthetic methodology outlined in Scheme 2 is found to be more problematic for anilines bearing a *para*-methyl substituent, such as $MesNH_2$ (Mes = 2,4,6-$Me_3C_6H_2$). Thus, the spirocyclic system **2** was unexpectedly isolated (rather than pro-ligand [**1**^{Mes}]H) when $MesNH_2$ was employed as the aniline reagent (Figures 1 and 4). The identity of **2** was unambiguously established by X-ray crystallography and is consistent with the assimilation of a single equivalent of $MesNH_2$, followed by ring closure to generate a quaternary carbon centre. Particularly remarkable is the activation of the *para*-methyl group of the mesityl ring, chemistry which is consistent with the appearance of alkenic CH_2 and CH resonances in the ^{1}H NMR spectrum of **2**, and with the disappearance of the *para*-CH_3 signal. Consistently, the C-C bond distances determined crystallographically for the six-membered ring are no longer equivalent, with the C2-C3, C4-C5, C5-C6 and C2-C7 separations ranging from 1.454(3) to 1.529(3) Å (consistent with descriptions as carbon-carbon single bonds),[11] and the C1-C2, C3-C4 and C6-C7 distances [1.351(4), 1.336(3) and 1.334(3) Å, respectively] are indicative of double bond character. Mechanistically, the formation of **2** necessitates initial uptake of a single equivalent of $MesNH_2$, followed by deprotonation at the mesityl *para*-CH_3 group thereby generating a C-based nucleophile, which (by virtue of resonance) attacks the second chloro-imine function through the *ipso*-carbon. While such a proposal has little literature precedent, it is entirely consistent with the notion that the related ortho-xylyl amine, 2,6-$Me_2C_6H_3NH_2$, does not undergo analogous spirocyclic ring closure, but instead generates the desired protio-ligand [**1**^{Xyl}]H in good yield (Scheme 3 and Figure 1).

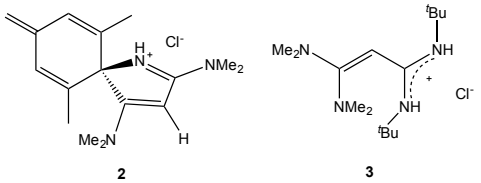

Figure 4. Spiro-cyclic compound **2** obtained from condensation chemistry utilising $MesNH_2$; rearranged product **3** obtained with ^{t}BuNH_2 under aqueous conditions.

The one-pot protocol can be extended to alkyl amines, such as ^{t}BuNH_2, although in this case the isolation of the desired pro-ligand [**1**^{tBu}]H necessitates an anhydrous work-up, followed by

sublimation, and suffers from a very poor yield (ca. 5%). [**1**^{tBu}]H isolated in this fashion has been characterized by multinuclear NMR spectroscopy and by mass spectrometry (including accurate mass measurement), with its existence as the diimine tautomer in solution being suggested by a methylene resonance integrating to two hydrogens at δ_H = 3.86 ppm (*cf.* 3.37 and 3.27 ppm for [**1**^{Ph}]H/[**1**^{Dipp}]H, respectively). However, the use of a more convenient aqueous work-up procedure similar to that employed for *N*-aryl substituted diimines [**1**^{Ph}]H, [**1**^{Xyl}]H and [**1**^{Dipp}]H, leads instead to the formation of the re-arranged amidinium chloride salt **3**, the identity of which was confirmed by standard spectroscopic/analytical methods and X-ray crystallography (Figures 1 and 4). The solid state structure is consistent with rearrangement of the amino-functions across the C_3 backbone, presumably mediated by reversible imine/iminium formation under aqueous conditions. Geometrically, **3** reveals a highly conjugated heavy atom skeleton, with the C-C [1.407(2) and 1.411(2) Å] and C-N bond distances [1.348(2) - 1.366(2) Å] falling in each case between the respective carbon-carbon and carbon-nitrogen single and double bond lengths.

Access to *N*-mesityl ligand systems requires the use of an alternative synthetic approach, in which the (N-nacnac)H protio-ligand is assembled via C-C bond formation from two pre-formed amidine components. Deprotonation of an *N*-aryl-*N′*,*N′*-dialkyl substituted amidine at the β-CH_2 position, followed by electrophilic quenching with ClC(NR)NR'$_2$ allows for the modular synthesis of a range of (N-nacnac)H systems (Scheme 4). Thus, [**1**^{Dipp}]H can be synthesized in this fashion, with the yield of the final step (ca. 35%) being comparable to that achieved in the condensation procedure outlined above. While the methodology outlined in Scheme 4 does require additional synthetic steps for the formation of the amidine precursors, it is of note that both components can be prepared from a common urea starting material of the type R(H)NC(O)NR'$_2$ (see SI). Moreover, the scope of this approach is such that systems bearing N-mesityl substituents, such as [**4**^{Mes}]H and backbone phenyl groups (e.g. [**5**^{Mes}]H) can be prepared in this way. Each of these systems has been characterized by conventional spectroscopic and analytical techniques, with crystallographic data obtained for [**4**^{Mes}]H in the solid state also confirming the presence of the diimine tautomer implied in solution by NMR measurements (Figure 1).

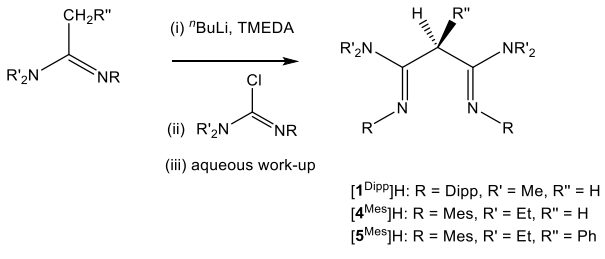

Scheme 4. C-C bond formation as a synthetic route to (N-nacnac)H protio-ligands.

Complexation studies. Having established routes to the target (N-nacnac)H protio-ligands, we then sought to establish viable synthetic approaches for a range of coordination complexes, ultimately with a view to comparing donor properties with more well established Nacnac analogues. With this in mind, we targeted (i) the use of metal alkyl reagents (M = Li, Mg, Al) to generate a range of metal N-nacnac complexes via deprotonation of the protio-ligands; and (ii) the use of such reagents in trans-metallation chemistry, targeting complexes of Sn^{II} (as an exemplar from the *p*-block) and Yb^{II} as examples of *f*-element complexes. The existence of the corresponding metal complexes featuring (backbone-Me) Nacnac ligands made these two platforms attractive from the perspective of like-for-like comparison.[13,14]

Accordingly, the reactions of (N-nacnac)H protio-ligands with ^{n}BuLi, for example, lead to deprotonation of the backbone methylene group and to the formation of the corresponding lithium complex of the conjugate base [N-nacnac]$^-$. Such chemistry can be carried out either in the presence or absence of a coordinating solvent, leading to the generation of either monomeric donor-stabilized complexes such as [**1**^{Dipp}]Li(OEt$_2$), or donor-free oligomeric systems such as {[**4**^{Mes}]Li}$_2$ (Scheme 5). In each case, the formation of an essentially planar six membered LiN_2C_3 chelate ring could be established definitively by X-ray crystallography, with the nearly identical C-N and C-C distances

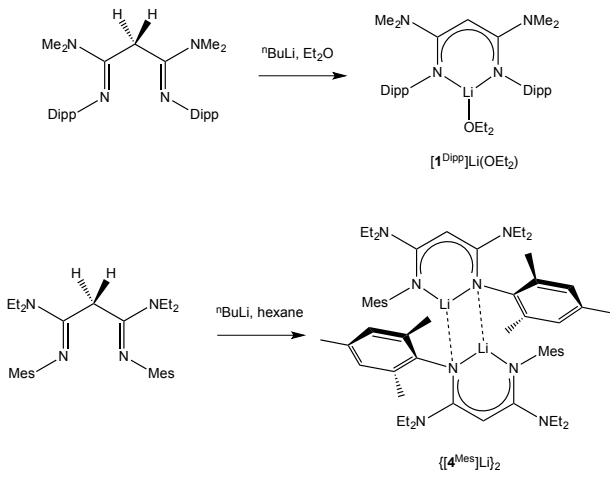

Scheme 5. Lithiation of (N-nacnac)H protio-ligands with ^{n}BuLi.

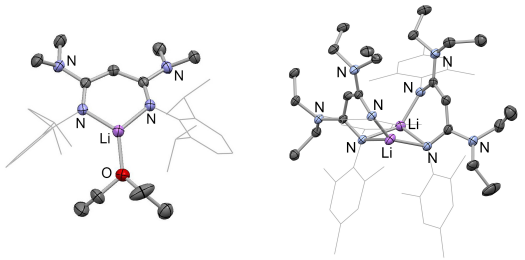

Figure 5. (left to right) Molecular structures of [**1**^{Dipp}]Li(OEt$_2$), and one of the molecules in the asymmetric unit of {[**4**^{Mes}]Li}$_2$, in the solid state as determined by X–ray crystallography. Displacement ellipsoids drawn at 50 % probability level; most H-atoms, minor disorder components and solvate molecules omitted and N-substituents drawn in wireframe format for clarity. Key metrical parameters are given in Table 3.

Table 3. Crystallographically determined bond lengths (Å) and angles (°) for N-nacnac and (N-nacnac)H complexes of lithium, magnesium and aluminium.

Complex	*d*(M1-N1),[a] *d*(M1-N2)	*d*(N1-C1), *d*(N2-C3)	*d*(C1-C2), *d*(C2-C3)	∠(N1-M1-N2)
[**1**^{Dipp}]Li(OEt$_2$)	1.908(4) 1.914(3)	1.321(3) 1.336(3)	1.409(2) 1.420(2)	101.4(2)
{[**4**^{Mes}]Li}$_2$[b]	1.927(5) 1.918(5) 2.062(5)[c] 2.063(5)[c] 2.075(5)[c] 2.065(5)[c]	1.346(3) 1.346(3) 1.357(3) 1.344(3)	1.408(3) 1.420(4) 1.410(3) 1.412(4)	101.5(2) 102.5(2)
[**1**^{Dipp}]MgI(OEt$_2$)[b]	2.036(2) 2.035(2)	1.358(3) 1.330(3)	1.396(2) 1.441(3)	98.7(1)
[**4**^{Mes}]MgI(OEt$_2$)	2.035(2) 2.026(2)	1.345(3) 1.352(3)	1.414(3) 1.409(3)	95.3(1)
{[**4**^{Mes}]H}MgI$_2$	2.082(3) 2.092(2)	1.319(5) 1.312(5)	1.533(4) 1.527(4)	91.6(1)
[**1**^{Ph}]AlMe$_2$	1.917(5) 1.906(8)	1.36(1) 1.36(1)	1.42(1) 1.42(1)	95.3(3)
[**1**^{Dipp}]AlMe$_2$	1.923(2) 1.923(2)	1.355(3) 1.344(3)	1.404(3) 1.422(3)	99.5(1)

[a] See Fig. 6 for atom numbering scheme. [b] Metric parameters given for one of the molecules in the asymmetric unit. [c] Associated with a bridging N atom.

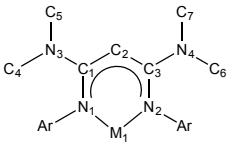

Figure 6. Atom numbering scheme used in Table 2.

within the ring [e.g. 1.321(3)/1.336(3) and 1.409(2)/1.420(2) Å for [**1**^{Dipp}]Li(OEt$_2$)] being consistent with a delocalized imino-amide formulation (Figure 5 and Table 3).[15]

Similar chemistry can also be effected using magnesium or aluminium alkyls (Scheme 6 and Figure 7); the reactions with either methyl Grignard reagents in diethyl ether or trimethyl-aluminium in toluene generate methane and [N-nacnac]$^-$ complexes featuring the respective metals in four-coordinate environments. As with the lithium complexes outlined above, metrical parameters for [**1**^{Dipp}]MgI(OEt$_2$), [**4**^{Mes}]MgI(OEt$_2$), [**1**^{Ph}]AlMe$_2$ and [**1**^{Dipp}]AlMe$_2$ are consistent with backbone deprotonation and with a delocalized imino-amide ligand description.[16,17] Thus for example, [**4**^{Mes}]MgI(OEt$_2$) features Mg-N, C-N and C-C distances within the metal chelate ring of 2.026(2)/2.035(2), 1.345(3)/1.352(3) and 1.409(3)/1.414(3) Å, respectively, while the related complex {[**4**^{Mes}]H}MgI$_2$ (obtained as a minor side-product in the synthesis of [**4**^{Mes}]MgI(OEt$_2$); see SI) which incorporates the fully protonated neutral ligand [**4**^{Mes}]H, features longer M-N and C-C [2.092(2)/2.082(3) and 1.527(4)/1.533(4) Å, respectively] and shorter N-C distances [1.312(5)/1.319(5) Å] consistent with a non-conjugated diimine formulation.

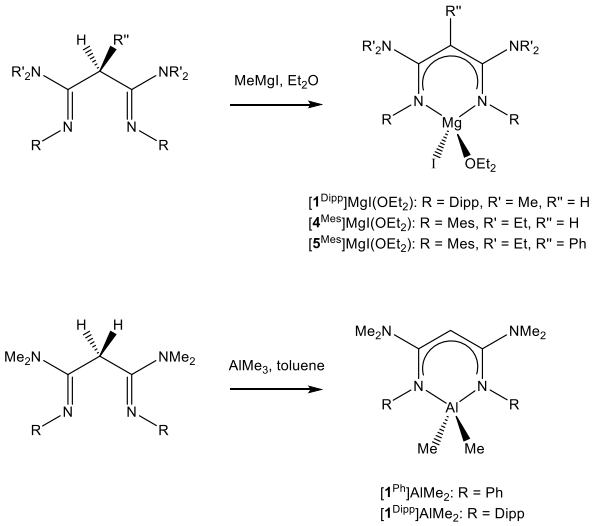

Scheme 6. Metallation of (N-nacnac)H protio-ligands with methyl-magnesium and -aluminium reagents.

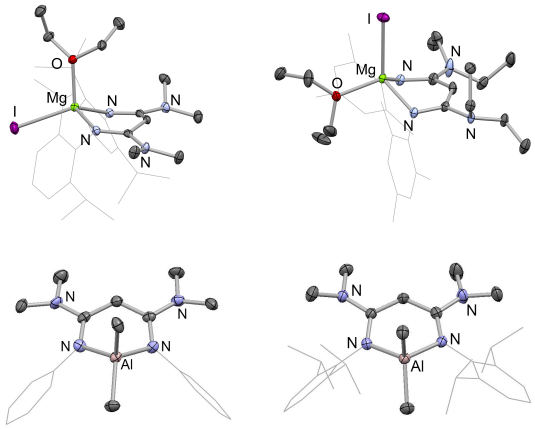

Figure 7. Molecular structures of (upper) [**1**^{Dipp}]MgI(OEt$_2$) (one of two molecules in the asymmetric unit) and [**4**^{Mes}]MgI(OEt$_2$), and (lower) [**1**^{Ph}]AlMe$_2$ and [**1**^{Dipp}]AlMe$_2$ in the solid state as determined by X–ray crystallography. Displacement ellipsoids drawn at 50 % probability level; most H-atoms, minor disorder components and solvate molecules omitted and N-substituents drawn in wireframe format for clarity. Key metrical parameters are given in Table 3.

Lithiated N-nacnac derivatives, either as isolated materials, or generated *in situ* from the corresponding protio-ligand and ^{n}BuLi, prove to be convenient reagents for trans-metallation chemistry, e.g., for the synthesis of Sn^{II} chloride and hydride complexes. Moreover, with a view to examining the effects of variation in the steric bulk of the N-bound aryl substituents, we targeted complexes featuring ligands **1**^{Ph}, **1**^{Xyl} and **1**^{Dipp} (Scheme 7). Yields of the respective metal complexes (of the type [**1**^{R}]MCl) range from 50-80%, and each has been characterized by standard spectroscopic techniques and by X-ray diffraction (Figure 8).

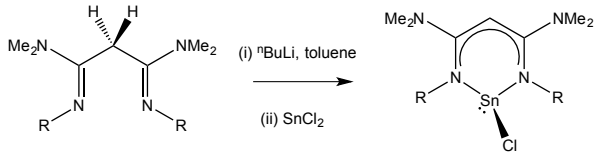

[1R]SnCl: R = Ph, Xyl, Dipp

Scheme 7. Syntheses of N-nacnac-supported Sn^{II} chloride complexes.

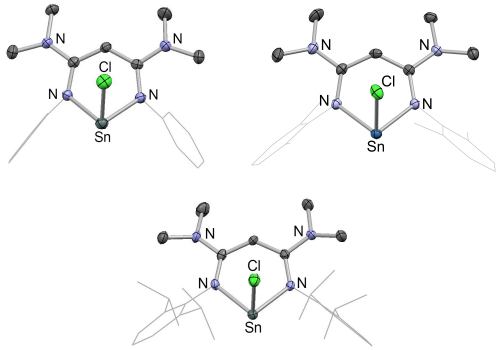

Figure 8. Molecular structures of [**1**^{Ph}]SnCl, [**1**^{Xyl}]SnCl and [**1**^{Dipp}]SnCl in the solid state as determined by X–ray crystallography. Displacement ellipsoids drawn at 50 % probability level; most H-atoms, minor disorder components and solvate molecules omitted and N-substituents drawn in wireframe format for clarity. Key metrical parameters are given in Table 4.

Table 4. Crystallographically determined bond lengths (Å) and angles (°) for tin N-nacnac complexes. For comparison, data given in square parentheses refer to the corresponding (backbone Me) Nacnac complexes featuring the same N-aryl substituents.[13]

Complex	*d*(M1-N1),[a] *d*(M1-N2)	*d*(N1-C1), *d*(N2-C3)	*d*(C1-C2), *d*(C2-C3)	∠(N1-M1-N2)
[**1**^{Ph}]SnCl	2.156(4) 2.156(4)	1.362(6) 1.368(7)	1.401(6) 1.406(5)	84.4(1)
	[2.170(9)] [2.174(9)]	[1.338(14)] [1.379(15)]	[1.348(17)] [1.453(17)]	[84.9(3)]
[**1**^{Xyl}]SnCl	2.156(3) 2.148(2)	1.354(4) 1.352(3)	1.405(3) 1.402(4)	86.4(1)
[**1**^{Dipp}]SnCl	2.167(4) 2.156(5)	1.355(7) 1.342(6)	1.410(8) 1.404(9)	89.8(2)
	[2.185(2)] [2.180(2)]	[1.329(3)] [1.344(3)]	[1.392(4)] [1.401(3)]	[85.2(1)]
[**1**^{Dipp}]SnH	2.190(3) 2.194(4)	1.338(5) 1.338(6)	1.401(7) 1.416(6)	89.4(7)
	[2.198(2)] [2.194(2)]	[1.326(3)] [1.326(3)]	[1.404(3)] [1.405(3)]	[85.1(1)]

[a] See Fig. 6 for atom numbering scheme. [b] Metric parameters given for one of the molecules in the asymmetric unit. [c] Associated with a bridging N atom.

The structures of these tin complexes allow for a systematic appraisal of the steric and electronic effects brought about by changes in the *N*-aryl substituents, and in particular as the bulk of the aryl group is increased in the order Ph < Xyl < Dipp.[13a-c] Thus, more 'puckered' complexes are associated with smaller aryl groups, as manifested by greater projection of the metal centre out of the least-squares plane defined by the NC_3N N-nacnac chelate ring (e.g. by 0.99 Å for [**1**^{Ph}]SnCl) and by a complementary displacement of the N-bound aryl groups below the same plane (with the *ipso*-carbons lying on average 0.91 Å out of plane for [**1**^{Ph}]SnCl). As the aryl groups become larger, mutual steric repulsion forces them apart (Figure 9) with the resulting disrotatory realignment of the N-M bonds dropping the metal centre closer to the NC_3N plane. Thus, in the sequentially bulkier systems [**1**^{Xyl}]SnCl and [**1**^{Dipp}]SnCl, for example, the metal centre lies 0.86 and 0.56 Å above the NC_3N plane, and the *ipso*-carbons are on average 0.68 and 0.52 Å below the plane. By means of comparison, the structure of the corresponding Nacnac system, {HC(MeCDippN)$_2$}SnCl features a Sn(II) centre which lies 0.66 Å out of the analogous ligand plane.[13c] These factors – notably the drive for the larger N-aryl groups to lie closer to the NC_3N plane on steric grounds - exert a secondary influence on the electronic properties of the [**1**^{Ph}]$^-$, [**1**^{Xyl}]$^-$ and [**1**^{Dipp}]$^-$ ligands. Increasing congestion in the NC_3N plane as the aryl groups become larger forces the *exo*-cyclic NMe_2 groups to rotate out of the plane. Thus, in [**1**^{Ph}]SnCl, [**1**^{Xyl}]SnCl and [**1**^{Dipp}]SnCl the torsion angles between the NC_3N chelate and NC_2 amino planes are 16.3/16.3°, 22.2/24.9° and 25.3/30.8°, respectively, implying less efficient π-conjugation into the chelate ring.

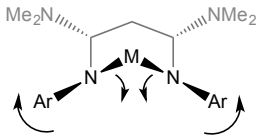

Figure 9. Structural realignment of the N-bound substituents of [N-nacnac]$^-$ ligands as the bulk of the aryl groups increases.

In broader terms, comparison of the structural parameters determined for [**1**^{R}]SnCl with the corresponding complexes of the more well-established Nacnac ligand family reveals small but significant differences. [**1**^{Dipp}]SnCl, for example shows with a marked widening of the N-Sn-N angle [89.8(2) vs. 85.2(1)°] and an associated shortening of the Sn-N distances [2.161 (mean) vs. 2.183 Å (mean)] compared to {HC(MeCDippN)$_2$}SnCl.[13c] Spectroscopically, the chemical shifts associated with the backbone γ-CH proton are also consistent with a more electron rich ligand framework in the N-nacnac complexes. The respective signals are shifted significantly upfield compared to their Nacnac analogues [e.g. 4.04 ppm for [**1**^{Dipp}]SnCl vs. 5.05 ppm for {HC(MeCDippN)$_2$}SnCl].[13c] Such an effect is consistent with the well-documented effects of π-donor amino groups on alkene resonances.[18]

The availability of the more sterically encumbered [**1**^{Dipp}]SnCl system allowed us to explore the possibilities for the synthesis of the corresponding tin hydride. Accordingly, treatment with K[Et$_3$BH] in toluene led to the formation of the corresponding metal hydride [**1**^{Dipp}]SnH, which has been characterized by spectroscopic and crystallographic methods (Scheme 8 and Figure 10). This compound is thermally fragile, showing signs of decomposition to tin metal over a period of ca. 12 h in C_6D_6

solution, and over a period of several days in the solid state. Spectroscopically, the ^{1}H and ^{119}Sn resonances for the Sn-H moiety (δ_H = 13.42 ppm; δ_{Sn} = -18 ppm) can be compared with the corresponding data obtained for {HC(MeCDippN)$_2$}SnH (δ_H = 13.96 ppm; δ_{Sn} = -4.5 ppm).[13d] While these differences are relatively small, divergence in the solid-state structures of the two compounds again hints at underlying electronic differences. Thus, while {HC(MeCDippN)$_2$}SnH exists as a weakly bound head-to-head dimer, featuring bridging Sn···H contacts of 4.01(3) Å and a Sn···Sn separation of 3.71 Å,[13d] [**1**^{Dipp}]SnH is more obviously monomeric in the solid state (Figure 10). Although the position of the tin-bound hydrogen atom could not be reliably established by X-ray crystallography, the alignment of the molecular units is in head-to-tail fashion, such that Sn-H···Sn interactions are precluded. Conceivably, this phenomenon signals a less polarized Sn-H bond, as a result of ligation by the more electron-rich N-nacnac ligand. Steric factors might also be expected to play a role, given the greater size of the backbone NMe$_2$ group (vs. Me), although this is presumably not a major factor, given that the distance between the centroids of the flanking Dipp rings changes little between the two systems.

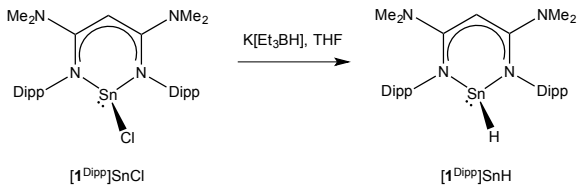

[**1**^{Dipp}]SnCl [**1**^{Dipp}]SnH

Scheme 8. Syntheses of a N-nacnac-supported Sn^{II} hydride.

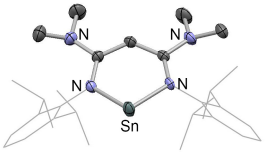

Figure 10. Molecular structure of [**1**^{Dipp}]SnH in the solid state as determined by X–ray crystallography. Displacement ellipsoids drawn at 50 % probability level; most hydrogen atoms, minor disorder components and solvate molecules omitted and N-substituents drawn in wireframe format for clarity. Key metrical parameters are given in Table 3.

While Nacnac ligands have been employed effectively across the Periodic Table, another area where they have found particularly widespread application is in *f*-element chemistry.[2,19,20] In part this reflects the combination of steric bulk and hard N-donor character allied to a chelating ligand framework. With this in mind, we sought to further benchmark our new N-nacnac ligands by synthesizing example of Yb^{II} complexes, which again offer for like-for-like comparison with existing Nacnac systems.[14] Thus, the reactions of *in situ* potassiated N-nacnac reagents with YbI$_2$·2(thf) were investigated (Scheme 9).

Assimilation of either one or two equivalents of the N-nacnac ligand is possible via iodide metathesis, leading to the formation of compounds of composition {[**1**^{Dipp}]Yb(μ-I)}$_2$ and [**1**^{Dipp}]$_2$Yb, respectively. Both compounds could be characterized by standard spectroscopic and analytical techniques, and their structures in the solid state determined by X-ray crystallography (Figure 11). Interestingly, while the structures determined for *s*- and *p*-block N-nacnac complexes reveal coordination modes which strongly resemble those of the related 'parent' Nacnac systems, those of {[**1**^{Dipp}]Yb(μ-I)}$_2$ and [**1**^{Dipp}]$_2$Yb show greater

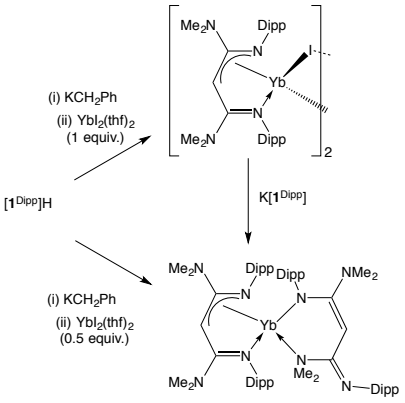

Scheme 9. Syntheses of homo- and heteroleptic Yb^{II} N-nacnac complexes.

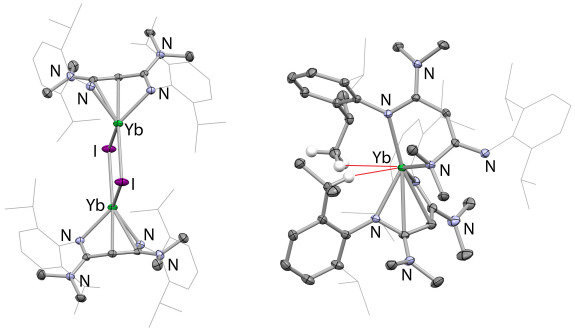

Figure 11. Molecular structures of {[**1**^{Dipp}]Yb(μ-I)}$_2$ and [**1**^{Dipp}]$_2$Yb in the solid state as determined by X–ray crystallography. Displacement ellipsoids drawn at 50 % probability level; most hydrogen atoms omitted and N-substituents drawn in wireframe format for clarity. The structure of {[**1**^{Dipp}]Yb(μ-I)}$_2$ is centrosymmetric; only one of the two independent components in the asymmetric unit is shown.

structural differences. {[**1**^{Dipp}]Yb(μ-I)}$_2$, for example, features an η^4 mode of coordination of the N-nacnac ligand involving close contacts with four of the five atoms of the N_2C_3 backbone [*d*(Yb-C) = 2.734(5), 2.811(5) Å; *d*(Yb-N) = 2.337(5), 2.336(4) Å, for one component of the asymmetric unit]. The other Yb···C contact is somewhat longer [2.961(5) Å], and a description in terms of an η^3-azaallyl interaction augmented by the N-coordination of a discrete imine donor (Scheme 8) is also in line with the N-C and C-C distances within the N-nacnac backbone. Thus, the C-N distance associated with the imine function [1.326(8) Å] is

shorter than that in the azaallyl unit [1.363(9) Å], and the C-C distance within the latter [1.383(8) Å] is shorter than the formal single bond which links the two donor components [1.455(7) Å]. The corresponding product of the reaction of $YbI_2(thf)_2$ with {HC(MeCDippN)$_2$}K, by contrast generates a dimeric complex of the type {(Nacnac)Yb(thf)(μ-I)}$_2$, featuring the more common η^2 *N,N'* mode of coordination of the β-diketiminate while retaining one molecule of thf at each metal centre.[14b] Such differences highlight the enhanced donor capabilities of the N-nacnac ligand variant, in this case through the direct involvement of the more electron rich ligand backbone.

The related *bis*(N-nacnac) complex [**1**^{Dipp}]$_2$Yb shows even greater structural divergence from its Nacnac counterpart. Thus, the solid-state structure (Figure 9) shows two distinct modes of coordination: one N-nacnac ligand is coordinated in η^4-fashion, similar to the mode of ligation seen in {[**1**^{Dipp}]Yb(μ-I)}$_2$ [*d*(Yb-C) = 2.741(2), 2.776(2), 2.925(2) Å; *d*(Yb-N) = 2.369(1), 2.385(1) Å], while the second ligand adopts a unique geometry, being bound to the metal through one NDipp unit and one of the 'backbone' NMe_2 groups. As such, a pendant imine function is projected away from the metal centre, which allows for an alternative (less sterically demanding) chelate geometry. The metal coordination environment is completed by two Yb···H-C contacts involving the hydrogens of isopropyl substituents from the two N-nacnac ligands. By contrast, the solid state structure of {HC(MeCDippN)$_2$}$_2$Yb reported by Harder features two identically bound *N,N'*-chelating Nacnac ligands [*d*(Yb-N) = 2.381(1), 2.399(1) Å] and a metal centre with a close to tetrahedral coordination geometry.[14a]

Conclusions

The synthesis of a new class of amino-functionalized β-diketiminato ligands (N-nacnacs) is reported, with two approaches having been developed to protio-ligands bearing backbone NMe_2 or NEt_2 groups and a range of N-bound aryl substituents. In contrast to their (Nacnac)H counterparts, the structures of these systems both in the solution and in the solid state feature the bis(imine) tautomer and a backbone CH_2 group.

Direct metallation with group 1, 2 or 13 metal alkyls allows access to the respective metal complexes via deprotonation of the methylene group. The structures of a range of Li, Mg and Al compounds have been determined, and in each case are consistent with a delocalized imino-amide ligand description. Transmetallation has then been explored using lithium N-nacnac complexes possessing varying steric profiles, with Sn^{II} compounds being targeted (via metathesis) in order to provide like-for-like comparison with the analogous Nacnac complexes. While analogies can be drawn between N-nacnac and Nacnac complexes along similar lines to those described previously for guanidinate/amidinate systems, the degree of electronic perturbation effected by introduction of the backbone NR_2 groups appears to be restricted (particularly for more bulky N-nacnac ligands) by the inability of the amino group to achieve effective conjugation with the N_2C_3 heterocycle. Much more radical divergence from the Nacnac structural norms are, however, observed in the complexes of the larger, harder Yb^{II} ion, with azaallyl/imino and even azaallyl/NMe_2 coordination modes being demonstrated by X-ray crystallography. Such observations hint at potential avenues for exploitation of this ligand family in the near future.

Experimental Section

General considerations

All manipulations were carried out using standard Schlenk line or dry-box techniques under an atmosphere of argon. Solvents were degassed by sparging with argon and dried by passing through a column of the appropriate drying agent using a commercially available Braun SPS. NMR spectra were measured in C_6D_6 or $CDCl_3$ which were dried over potassium or molecular sieves, respectively, and stored under argon in a Teflon valve ampoule. NMR samples were prepared under argon in 5 mm Wilmad 507-PP tubes fitted with J. Young Teflon valves. NMR spectra were measured on Varian Mercury-VX-300 or Bruker AVII-500 spectrometers; ^{1}H and ^{13}C NMR spectra were referenced internally to residual protio-solvent (^{1}H) or solvent (^{13}C) resonances and are reported relative to tetramethylsilane (δ = 0 ppm). ^{7}Li, ^{27}Al and ^{119}Sn NMR spectra were referenced with respect to LiCl/D_2O, $Al(H_2O)_6^{3+}$ and $SnMe_4$, respectively. Chemical shifts are quoted in δ (ppm) and coupling constants in Hz. Elemental analyses were carried out at London Metropolitan University. The syntheses of $MesNC(Cl)NEt_2$, $MesNC(Me)NEt_2$, $MesNC(CH_2Ph)NEt_2$, $DippNC(Cl)NMe_2$, $DippNC(Me)NMe_2$, **2** and **3** are described in the supporting information.

Syntheses of novel compounds

Generic synthesis of protio-ligands [1^R]H via route (i): To a solution of dichloromethylene-dimethylammonium chloride (15.00 g, 92.3 mmol) in dichloromethane (100 mL) was added dropwise *N,N*-dimethylacetamide (4.10 mL, 44.1 mmol) at room temperature, and the reaction mixture refluxed for 6 h. After the removal of volatiles *in vacuo*, chloroform was added (100 mL), followed by $ArNH_2$ (100 mmol) via syringe at 0°C. The reaction mixture was then refluxed for 12 h. After cooling to room temperature, saturated KOH solution was added at 0°C until the pH was ≥ 10, followed by water (100 mL). The aqueous layer was washed twice with chloroform (100 mL each) and the organic layer extracted, washed with brine (100 mL) and dried over $MgSO_4$. The resulting solution was filtered and volatiles removed *in vacuo* to give the crude product. **[1^{Ph}]H**: The solid crude product was washed with cold hexane to yield a yellow solid as a spectroscopically pure material. Yield: 7.55 g, 56%. Crystals suitable for X-ray crystallography were obtained from a saturated acetone solution at -26°C. ^{1}H NMR (400 MHz, $CDCl_3$): δ_H 2.84 (s, 12H, $(CH_3)_2N$), 3.37 (s, 2H, N-nacnac backbone CH_2), 6.57 (d, $^3J_{HH}$ = 7.7 Hz, 4H, *o*-CH of Ph), 6.90 (t, $^3J_{HH}$ = 7.4 Hz, 2H, *p*-CH of Ph), 7.18 (t, $^3J_{HH}$ = 7.6 Hz, 4H, *m*-CH of Ph). ^{13}C{^{1}H} NMR (100 MHz, $CDCl_3$): δ_C 29.4 (N-nacnac backbone CH_2), 38.6 ($(CH_3)_2N$), 122.0 (*p*-CH of Ph), 122.7 (*o*-CH of Ph), 129.1 (*m*-CH of Ph), 150.8 and 155.6 (*ipso*-C of Ph and imine quaternary C). ESI-MS (*m/z*, %): 309.2, weak, $[M+H]^+$; accurate mass: calc. for $C_{19}H_{25}N_4$ ($[M+H]^+$) 309.2074, meas. 309.2075. Elemental microanalysis: calc. for $C_{19}H_{24}N_4$: C 73.99, H 7.84, N 18.17%, meas. C 74.13, H 8.01, N 18.00%. Crystallographic data: $C_{19}H_{24}N_4$, M_r = 308.43, trigonal, *R*-3, *a* = 26.6569(4), *b* = 26.6569(4), *c* = 12.9106(3) Å, *V* = 7945.0(2) Å^3, *Z* = 18, ρ_c = 1.160 g cm^{-3}, *T* = 150 K, λ = 1.54180 Å. 10753 reflections collected, 3694 independent [R(int) = 0.077] used in all calculations. R_1 = 0.0419, wR_2 = 0.1072 for observed unique reflections [$I > 2\sigma(I)$] and R_1 = 0.0451, wR_2 = 0.1110 for all unique reflections. Max. and min. residual electron densities 0.25 and -0.27 e Å^{-3}. CCDC ref:

1528016. **[1^{Xyl}]H**: (NB. additional base (*N*-ethyl diisopropyl amine, 11.70 mL, 68.36 mmol) was added along with the aniline for the second reflux step). The product was recrystallized from minimal acetone:hexane as pale yellow crystals; additional crops could be obtained from the filtrate to give an overall yield of 5.67 g (35%). ^{1}H NMR (400 MHz, $CDCl_3$): δ_H 1.98 (s, 12H, CH_3 of Xyl), 2.86 (s, 12H, $(CH_3)_2N$), 3.13 (s, 2H, N-nacnac backbone CH_2), 6.80 (t, $^3J_{HH}$ = 9.1 Hz, 2H, *p*-CH of Xyl), 6.98 (d, $^3J_{HH}$ = 7.4 Hz, 4H, *m*-CH of Xyl). $^{13}C\{^1H\}$ NMR (100 MHz, $CDCl_3$): δ_C 18.6 (CH_3 of Xyl), 31.4 (N-nacnac backbone CH_2), 38.6 ($(CH_3)_2N$), 121.6 (*p*-CH of Xyl), 128.0 (*m*-CH of Xyl), 128.9 (*o*-C of Xyl), 147.9 (*ipso*-C of xyl), 154.1 (imine quaternary C). ESI-MS (*m*/*z*, %): 365, weak, $[M+H]^+$; accurate mass: calc. for $C_{23}H_{33}N_4$ 365.2700, meas. 365.2698. Elemental microanalysis: calc. for $C_{23}H_{32}N_4$: C 75.78, H 8.85, N 15.37%, meas. C 75.65, H 9.01, N 15.25. Crystallographic data: $C_{23}H_{32}N_4$, M_r = 364.53, tetragonal, *P* 4_32_12, *a* = 8.0421(1), *b* = 8.0421(1), *c* = 32.9265(6) Å, *V* = 2129.53(5) Å^3, *Z* = 4, ρ_c = 1.137 g cm^{-3}, *T* = 150 K, λ = 0.71073 Å. 4485 reflections collected, 1510 independent [R(int) = 0.035] used in all calculations. R_1 = 0.0428, wR_2 = 0.1087 for observed unique reflections [$I > 2\sigma(I)$] and R_1 = 0.0592, wR_2 = 0.1291 for all unique reflections. Max. and min. residual electron densities 0.22 and -0.24 e Å^{-3}. CCDC ref: 1528018. **[1^{Dipp}]H**: (NB. additional base (*N*-ethyl diisopropyl amine, 26.53 mL, 155 mmol) was added along with the aniline for the second reflux step). The crude product (a dark red oil) was dissolved in an acetone/hexane mixture and stirred vigorously for 10 min. Filtration followed by storage at -26°C overnight yielded the product as pale yellow crystals. Yield: 6.91 g, 33%. ^{1}H NMR (400 MHz, C_6D_6): δ_H 1.12 (d, $^3J_{HH}$ = 7.1 Hz, 12H, $(C\underline{H}_3)_2CH$), 1.18 (d, $^3J_{HH}$ = 7.1 Hz, 12H, $(C\underline{H}_3)_2CH$), 2.68 (s, 12H, $(CH_3)_2N$), 2.95 (br sept, $^3J_{HH}$ = ca. 7 Hz, 4H, $(CH_3)_2C\underline{H}$), 3.21 (s, 2H, N-nacnac backbone CH_2), 7.05 (t, $^3J_{HH}$ = 7.5 Hz, 2H, *p*-CH of Dipp), 7.12 (d, $^3J_{HH}$ = 7.5 Hz, 4H, *m*-CH of Dipp). $^{13}C\{^1H\}$ NMR (125 MHz, C_6D_6): δ_C 22.5 ($(\underline{C}H_3)_2CH$), 24.4 ($(\underline{C}H_3)_2CH$-), 28.6 ($(CH_3)_2\underline{C}H$), 32.0 (N-nacnac backbone CH_2), 38.5 ($(\underline{C}H_3)_2N$), 122.7 (*p*-CH of Dipp), 123.2 (*m*-CH of Dipp), 138.6 (*o*-C of Dipp), 146.0 (*ipso*-C of Dipp), 153.8 (imine quaternary C). ESI-MS (*m*/*z*, %): 477.4, 100, $[M+H]^+$; accurate mass: calc. for $C_{31}H_{49}N_4$ ($[M + H]^+$) 477.3952, meas. 477.3949. Elemental microanalysis: calc. for $C_{31}H_{48}N_4$: C 78.10, H 10.15, N 11.75%, meas. C 78.27, H 10.06, N 11.85%. Crystallographic data: $C_{31}H_{48}N_4$, M_r = 476.75, monoclinic, *P* $2_1/c$, *a* = 9.5453(1), *b* = 17.5799(2), *c* = 17.3757(2) Å, β = 91.7380(5)°, *V* = 2914.40(6) Å^3, *Z* = 4, ρ_c = 1.086 g cm^{-3}, *T* = 150 K, λ = 0.71073 Å. 12578 reflections collected, 6636 independent [R(int) = 0.019] used in all calculations. R_1 = 0.0480, wR_2 = 0.1132 for observed unique reflections [$I > 2\sigma(I)$] and R_1 = 0.0637, wR_2 = 0.1315 for all unique reflections. Max. and min. residual electron densities 0.28 and -0.27 e Å^{-3}. CCDC ref: 1528010.

[1^{tBu}]H: To a dichloromethane solution of dichloromethylene-dimethylammonium chloride (7.50 g, 46.15 mmol) was added dropwise at room temperature *N*,*N*-dimethylacetamide (2.05 mL, 22.05 mmol), and the reaction mixture refluxed for 12 h. After removal of volatiles *in vacuo*, chloroform was added, followed by *N*-ethyldiisopropylamine (11.70 mL, 68.36 mmol) and *tert*-butylamine (5.24 mL, 50 mmol) - both dropwise via syringe at 0 °C. The reaction mixture was then refluxed for a further 12 h. After allowing the solution to cool to room temperature, the solvent was removed *in vacuo* to give an orange solid, and the flask brought into the glovebox where it could be opened and a spatula used to break up the solid as much as possible. Subsequently, diethyl ether (100 mL) was added and the solution stirred overnight. After filtration, the solvent removed *in vacuo* to give a pale yellow spectroscopically pure solid. Yield: 0.24 g, 4% yield. ^{1}H NMR (400 MHz, C_6D_6) δ_H 1.36 (s, 18H, $C(CH_3)_3$), 2.43 (s, 12H, $(CH_3)_2N$), 3.86 (s, 2H, N-nacnac backbone CH_2). $^{13}C\{^1H\}$ NMR (101 MHz, C_6D_6) δ_C 29.9 (CH_3 of ^{t}Bu), 29.9 (N-nacnac backbone CH_2), 35.8 ($(CH_3)_2N$), 50.5 (quaternary C of ^{t}Bu), 157.4 (imine quaternary C). ESI-MS (*m*/*z*, %): 269, WEAK, $[M+H]^+$; accurate mass: calc. for $C_{15}H_{32}N_4$ 269.2700, meas. 269.2686.

Synthesis of [1^{Dipp}]H via route (ii): To a solution of DippNC(Me)NMe_2 (1.00 g, 4.06 mmol) was added ^{n}BuLi (2.66 mL of a 1.6 M solution in hexane, 4.26 mmol) and TMEDA (0.52 g, 0.665 mL, 4.46 mmol) in hexane (40 mL) at –78 °C. The reaction mixture was allowed to warm to room temperature and stirred for 30 min, then cooled to –78 °C. In a separate flask, DippNC(Cl)NMe_2 (1.08 g, 4.06 mmol) was dissolved in hexane (5 mL) and the resulting solution added dropwise to the reaction mixture. After the addition, the mixture was allowed to warm to room temperature, and stirred for 12 h. After heating at a gentle reflux for 1 h, and cooling to room temperature, water (5 mL) was slowly added to the reaction mixture, followed by dichloromethane (10 mL). The organic fraction was then washed with water (2 x 10mL) and aqueous sodium bicarbonate (10 mL, saturated). The organic fraction was dried ($MgSO_4$) and concentrated. The residue was recrystallised from boiling ethanol (10 mL) to give the product as a colourless solid. Yield: 0.69 g, 35%. Spectroscopic and analytical data matched those measured for a sample obtained via route (i).

[4^{Mes}]H was prepared from MesNC(Me)NEt_2 and MesNC(Cl)NEt_2 via route (ii) in an analogous manner to that described above, and the crude residue recrystallised from ethanol to give the product as a colourless crystalline solid. Yield: 66% on a 1 - 2g scale. ^{1}H NMR (400 MHz, C_6D_6): δ_H 0.98 (br s, 12H, $NCH_2C\underline{H}_3$), 2.07 (s, 12H, *o*-CH_3 of Mes), 2.21 (s, 6H, *p*-CH_3 of Mes), 3.18 (br s, 8H, $NC\underline{H}_2CH_3$), 3.31 (s, 2H, N-nacnac backbone CH_2), 6.88 (s, 4H, m-CH of Mes). $^{13}C\{^1H\}$ NMR (101 MHz, C_6D_6): δ_C 13.1 ($NCH_2\underline{C}H_3$), 18.4, 20.5 (CH_3 of Mes), 29.9 (N-nacnac backbone CH_2), 41.6 ($N\underline{C}H_2CH_3$), 128.5, 128.9, 130.1, 145.6 (Mes) 153.2 (imin quaternary C). EI-MS (*m*/*z*, %): 449.3, 100, $[M+H]^+$; accurate mass: calc. for $C_{29}H_{45}N_4^+$ ($[M+H]^+$) 449.3639, meas. 449.3641. Elemental microanalysis: calc. for $C_{29}H_{44}N_4$: C 78.10, H 10.15, N 11.75%; meas.: C 78.25, H 10.27, N 11.66%. Crystallographic data: $C_{29}H_{44}N_4$, M_r = 448.68, monoclinic, C 2/c, a = 12.142(2), b = 20.507(4), c = 10.584(2) Å, β = 91.35(3)°, V = 2634.6(9) Å^3, Z = 4, ρ_c = 1.131 g cm^{-3}, *T* = 100 K, λ = 0.71090 Å. 9834 reflections collected, 2453 independent [R(int) = 0.082] used in all calculations. R_1 = 0.0546, wR_2 = 0.1418 for observed unique reflections [$I > 2\sigma(I)$] and R_1 = 0.0597, wR_2 = 0.1461 for all unique reflections. Max. and min. residual electron densities 0.58 and -0.28 e Å^{-3}. CCDC ref: 1528020.

[5^{Mes}]H: To a solution of MesNC(CH_2Ph)NEt_2 (2.47 g, 8.00 mmol) in Et_2O (20 mL) was added TMEDA (0.93 g, 1.2 mL, 8.0 mmol) and the solution cooled to –78 °C. ^{n}BuLi (5.5 mL of a 1.6 M solution in hexane, 8.80 mmol) was then added and the reaction mixture warmed to room temperature, resulting in a yellow heterogeneous mixture. After stirring for a further 2 h, the mixture was cooled to –78 °C and MesNC(Cl)NEt_2 (2.0 g, 1.7 mL, 8.00 mmol) added. The reaction mixture was again warmed to room temperature, stirred for 16 and then refluxed for 1 h. After cooling to room temperature, water (10 mL) was added followed by dichloromethane (10 mL). The organic layer was extracted and washed with water (2 x 10 mL) and aqueous sodium bicarbonate (10 mL). The organic fraction was dried over $MgSO_4$ and concentrated to yield an orange oil, which was recrystallised from ethanol to give the product as colourless crystalline material Yield: 2.80 g, 66% yield. ^{1}H NMR (500 MHz, 298 K, C_6D_6): δ_H 0.70 (br, 12H, $NCH_2C\underline{H}_3$), 2.24 (s, 6H, CH_3 of Mes), 2.33 (s, 6H, CH_3 of Mes), 2.38 (s, 6H, CH_3 of Mes), 2.99 (v br, 8H, $NC\underline{H}_2CH_3$), 5.38 (s, 1H, N-nacnac backbone C$\underline{H}$Ph), 6.84 (s, 2H, *m*-CH of Mes), 6.88 (s, 2H, *m*-CH of Mes), 7.06 (t, $^3J_{HH}$ = 7.6 Hz, 1H, *p*-CH of Ph), 7.20 (t, $^3J_{HH}$ = 7.6 Hz, 2H, *p*-CH of Ph), 7.65 (d, $^3J_{HH}$ = 7.6 Hz, 2H, *m*-CH of Ph).^{1}H NMR (300 MHz, 298 K, $CDCl_3$): δ_H 0.74 (t, $^3J_{HH}$ = 7.0 Hz, 12H, $NCH_2C\underline{H}_3$), 2.13 (s, 6H, CH_3 of Mes), 2.18 (s, 6H, CH_3 of Mes), 2.20 (s, 6H, CH_3 of Mes), 3.04 (br m, 8H, $NC\underline{H}_2CH_3$), 5.16 (s, 1H, N-nacnac backbone C$\underline{H}$Ph), 6.73 (s, 2H, *m*-CH of Mes), 6.76 (s, 2H, *m*-CH of Mes), 7.21 (t, $^3J_{HH}$ = 7.6 Hz, 1H, *p*-CH of Ph), 7.30 (t, $^3J_{HH}$ = 7.6 Hz, 2H, *o*-CH of Ph), 7.49 (d, $^3J_{HH}$ = 7.6 Hz, 2H, *m*-CH of Ph). ^{1}H NMR (300 MHz, 333K,

$CDCl_3$): δ_H 0.76 (t, $^3J_{HH}$ = 7.0 Hz, 12H, $NCH_2C\underline{H}_3$), 2.11 (s, 6H, CH_3 of Mes), 2.17 (s, 6H, CH_3 of Mes), 2.19 (s, 6H, CH_3 of Mes), 3.04 (d m, $^3J_{HH}$ = 7.5 Hz, 8H, $NC\underline{H}_2CH_3$), 5.18 (s, 1H, N-nacnac backbone C<u>H</u>Ph), 6.72 (s, 2H, *m*-CH of Mes), 6.75 (s, 2H, *m*-CH of Mes), 7.18 (t, $^3J_{HH}$ = 7.6 Hz, 1H, *p*-CH of Ph), 7.28 (t, $^3J_{HH}$ = 7.6 Hz, 2H, *o*-CH of Ph), 7.48 (d, $^3J_{HH}$ = 7.6 Hz, 2H, *m*-CH of Ph). $^{13}C\{^1H\}$ NMR (121 MHz, 298K, C_6D_6): δ_C 13.2 ($NCH_2\underline{C}H_3$), 19.8, 20.5 (CH_3 of Mes), 20.6 (N-nacnac backbone <u>C</u>HPh), 43.3 ($N\underline{C}H_2CH_3$), 126.5 (Ph), 127.2 (Mes), 128.2 (Mes), 128.5 (Ph), 128.7 (Ph), 128.9 (Mes), 129.4 (Ph), 139.9 (Mes), 146.3 (imine quaternary C). EI-MS, (*m*/*z*, %): 524.4, 3, $[M]^+$; 509.5, 13, $[M\text{-}CH_3]^+$. Elemental microanalysis: calc. for $C_{34}H_{48}N_4$: C 80.10, H 9.22, N 10.68%; meas. C 79.89, H 9.37, N 10.57%.

[1^{Dipp}]Li(OEt$_2$): To a solution of [**1**^{Dipp}]H (2.00 mmol) in Et_2O (25 mL) at -78 ^{0}C was added a solution of ^{n}BuLi in hexane (0.88 mL of a 2.5 M solution, 2.20 mmol); the reaction mixture was warmed to room temperature and stirred for 12 h. Concentration to *ca.* 5 mL and storage at -26^{o}C yielded colourless crystals of the product as an analytically pure material. Yield 0.69 g, 62%. ^{1}H NMR (400 MHz, C_6D_6): δ_H 0.54 (t, $^3J_{HH}$ = 7.0 Hz, 6H, $C\underline{H}_3CH_2O$), 1.20 (d, $^3J_{HH}$ = 7.2 Hz, 12H, $(C\underline{H}_3)_2CH$), 1.31 (d, $^3J_{HH}$ = 6.8 Hz, 12H, $(C\underline{H}_3)_2CH$), 2.52 (s, 12H, $(C\underline{H}_3)_2N$), 2.64 (q, $^3J_{HH}$ = 7.1 Hz, 4H, $CH_3C\underline{H}_2O$), 3.51 (sept, $^3J_{HH}$ = 6.8 Hz, 4H, $(CH_3)_2C\underline{H}$), 4.09 (s, 1H, N-nacnac backbone CH), 7.03 (t, $^3J_{HH}$ = 7.4 Hz, 2H, *p*-CH of Dipp), 7.15 (d, $^3J_{HH}$ = 7.6 Hz, 4H, *m*-CH of Dipp).$^{13}C\{^1H\}$ NMR (100 MHz, C_6D_6): δ_C 13.6 ($\underline{C}H_3CH_2O$), 23.7 (($\underline{C}H_3)_2CH$), 25.4 (($\underline{C}H_3)_2CH$), 28.1 ($(CH_3)_2\underline{C}H$), 41.3 (($\underline{C}H_3)_2N$), 62.8 ($CH_3\underline{C}H_2O$), 72.8 (N-nacnac backbone CH), 121.7 (*p*-CH of Dipp), 123.7 (*m*-CH of Dipp), 141.1 (*o*-C of Dipp), 149.5 (*ipso*-C of Dipp), 166.2 (imine quaternary C). Crystallographic data: $C_{35}H_{57}LiN_4O$, M_r = 556.80, monoclinic, *P* 2$_1$/*n*, *a* = 9.80960(10), *b* = 25.6135(3), *c* = 14.2229(2) Å, β = 106.501(1)^o, *V* = 3426.44(5) Å^3, *Z* = 4, ρ_c = 1.079 g cm^{-3}, *T* = 150 K, λ = 0.71073 Å. 14549 reflections collected, 7740 independent [R(int) = 0.025] used in all calculations. R_1 = 0.0573, wR_2 = 0.1200 for observed unique reflections [$I > 2\sigma(I)$] and R_1 = 0.0807, wR_2 = 0.1409 for all unique reflections. Max. and min. residual electron densities 0.71 and -0.45 e Å^{-3}. CCDC ref: 1528011.

{[4^{Mes}]Li}$_2$: To a solution of [**4**^{Mes}]H (0.8 g, 1.8 mmol) in hexane (20 mL) at -78^{o}C was added ^{n}BuLi (1.23 mL of a 1.6 M solution, 1.96 mmol). The reaction mixture was warmed to room temperature and stirred for 16 h. After filtration, concentration and cooling to 4^{o}C a pale yellow crystalline material was obtained. Yield: 0.67 g, 81%. Crystals suitable for X-ray crystallography were grown from a hexane solution stored at +5 °C. ^{1}H NMR (C_6D_6, 300 MHz): δ_H 0.87 (t, $^3J_{HH}$ = 6.8 Hz, 12H, $NCH_2C\underline{H}_3$), 2.18 (s, 12H, *o*-CH_3 of Mes), 2.31 (s, 6H, *p*-CH_3 of Mes), 2.98 (q, $^3J_{HH}$ = 6.8 Hz, 8H, $NC\underline{H}_2CH_3$), 4.07 (s, 1H, N-nacnac backbone CH), 6.93 (s, 4H, m-CH of Mes). $^{13}C\{^1H\}$ NMR (C_6D_6, 101 MHz): δ_C 12.3 ($NCH_2\underline{C}H_3$), 19.3 (CH_3 of Mes), 20.8 (CH_3 of Mes), 42.8 ($N\underline{C}H_2CH_3$), 77.1 (N-nacnac backbone CH), 128.9 (Mes), 129.2 (Mes), 130.6 (Mes), 149.7 (Mes), 166.7 (imine quaternary C). ^{7}Li NMR (C_6D_6, 156 MHz): δ_{Li} 0.43. EI-MS (*m*/*z*, %): 454.4, 2 $[M]^+$; 448.5, 21, $[M\text{-Li+H}]^+$; 433.4, 79, $[M\text{-Li-}CH_3]^+$. The highly air-sensitive nature of {[**4**^{Mes}]Li}$_2$ meant that reliable microanalysis proved impossible to obtain. Crystallographic data: $C_{58}H_{88}Li_2N_8$, M_r = 909.23, triclinic, *P*-1, *a* = 13.617(3), *b* = 19.395(4), *c* = 22.395(5) Å, α = 75.23(3), β = 72.90(3), γ = 78.96(3)^o, *V* = 5422.6(19) Å^3, *Z* = 4, ρ_c = 1.114 g cm^{-3}, *T* = 100 K, λ = 0.71080 Å. 92884 reflections collected, 20768 independent [R(int) = 0.084] used in all calculations. R_1 = 0.0644, wR_2 = 0.1655 for observed unique reflections [$I > 2\sigma(I)$] and R_1 = 0.0906, wR_2 = 0.1849 for all unique reflections. Max. and min. residual electron densities 1.18 and -0.48 e Å^{-3}. CCDC ref: 1528023.

[1^{Dipp}]MgI(OEt$_2$): MeMgI (0.90 mL of a 1.10 M solution in diethyl ether, 0.99 mmol) was added dropwise to a solution of [**1**^{Dipp}]H (0.40 g, 0.825 mmol) also in diethyl ether (10 mL) at 0°C. The reaction mixture was warmed to room temperature and stirred for 30 min. The product was isolated as a white solid by filtration. Yield: 0.35 g, 50%. Single crystals suitable for X-ray diffraction were obtained from diethyl ether. ^{1}H NMR (400 MHz, C_6D_6): δ_H 0.46 (br, 6H, $OCH_2C\underline{H}_3$), 1.28 (br, 24H, $(C\underline{H}_3)_2CH$), 2.30 (s, 12H, $N(CH_3)_2$), 3.51 (b, 4H, $(CH_3)_2C\underline{H}$), 3.56 (s, 1H, N-nacnac backbone CH), 4.10 (br, 4H, $OC\underline{H}_2CH_3$), 7.14 (m, 6H, CH of Dipp). $^{13}C\{^1H\}$ NMR (100 MHz, C_6D_6): δ_C 11.3 ($OCH_2\underline{C}H_3$), 24.2 (($\underline{C}H_3)_2CH$), 26.8 (($\underline{C}H_3)_2CH$), 28.5 ($(CH_3)_2\underline{C}H$), 28.1 ($(CH_3)_2\underline{C}H$), 41.1 ($N(\underline{C}H_3)_2$), 60.0 (br, $O\underline{C}H_2CH_3$), 74.6 (N-nacnac backbone CH), 123.8 (br, Dipp), 124.5 (br, Dipp), 142.7 (Dipp), 145.4 (Dipp), 164.4 (imine quaternary C). EI-MS (*m*/*z*, %): 583.4, 100, $[M\text{-}Et_2O\text{-}\{(CH_3)_2CH\}]^+$. Elemental microanalysis: calc. for $C_{35}H_{57}N_4MgO$: C 59.96, H 8.20, N 7.99%; meas.: C 59.19, H 7.41, N 8.67%. Crystallographic data: $C_{35}H_{57}IMgN_4O$, M_r = 701.06, triclinic, *P*-1, *a* = 11.027(1), *b* = 16.357(1), *c* = 21.692(1) Å, α = 104.37(1) β = 93.58(1), γ = 105.64(1)^o, *V* = 3614.7(2) Å^3, *Z* = 4, ρ_c = 1.288 g cm^{-3}, T = 100 K, λ = 0.71073 Å. 53066 reflections collected, 14178 independent [R(int) = 0.026] used in all calculations. R_1 = 0.0274, wR_2 = 0.0648 for observed unique reflections [$I > 2\sigma(I)$] and R_1 = 0.0405, wR_2 = 0.0726 for all unique reflections. Max. and min. residual electron densities 0.57 and -0.38 e Å^{-3}. CCDC ref: 1528012.

[4^{Mes}]MgI(OEt$_2$): MeMgI (2.99 mL of a 1.1 M solution in diethyl ether, 7.92 mmol) was added to a solution of [**4**^{Mes}]H (2.96 g, 6.60 mmol) also in diethyl ether (30 mL) at 0°C. The reaction mixture was allowed to warm to room temperature and stirred for 30 min. The product was isolated as a white solid by filtration (3.05 g, 75 % yield). ^{1}H NMR (400 MHz, C_6D_6): δ_H 0.40 (br t, $^3J_{HH}$ = 6.8 Hz, 6H, $OCH_2C\underline{H}_3$), 0.82 (t, $^3J_{HH}$ = 7.2 Hz, 12H, $NCH_2C\underline{H}_3$), 2.12 (s, 6H, CH_3 of Mes), 2.24 (s, 6H, CH_3 of Mes), 2.78 (s, 6H, CH_3 of Mes), 2.94 (br q, $^3J_{HH}$ = 6.8 Hz, 4H, $NC\underline{H}_2CH_3$), 3.04 (br q, $^3J_{HH}$ = 7.0 Hz, 4H, $NC\underline{H}_2CH_3$), 3.27 (q, ^{3}J = 7.2 Hz, 4H, $OC\underline{H}_2CH_3$), 4.18 (s, 1H, N-nacnac backbone CH), 6.79 (s, 2H, *m*-CH of Mes), 6.82 (s, 2H, *m*-CH of Mes). $^{13}C\{^1H\}$ NMR (100 MHz, C_6D_6): δ_C 11.1 ($OCH_2\underline{C}H_3$), 11.3 ($NCH_2\underline{C}H_3$), 18.3 (CH_3 of Mes), 19.4 (CH_3 of Mes), 21.8 (CH_3 of Mes), 41.4 ($N\underline{C}H_2CH_3$), 63.3 ($O\underline{C}H_2CH_3$), 75.6 (N-nacnac backbone CH), 128.3 (Mes), 128.4 (Mes), 129.5 (Mes), 129.6 (Mes), 131.0 (Mes), 145.3 (Mes), 167.4 (imine quaternary C). EI-MS (*m*/*z*, %), 599.1, 1, $[M\text{-}Et_2O\text{+H}]^+$. Elemental microanalysis: calc. for $C_{33}H_{53}IMgN_4O$: C 58.89, H 7.94, N 8.32%; meas.: C 58.69, H 7.76, N 8.36%. Crystallographic data: $C_{33}H_{53}IMgN_4O$, M_r = 673.00, monoclinic, *P*2$_1$/*c*, *a* = 8.443(2), *b* = 40.607(8), *c* = 9.968(2) Å, β = 101.82(3)^o, *V* = 3345.1(12) Å^3, *Z* = 4, ρ_c = 1.336 g cm^{-3}, *T* = 100 K, λ = 0.71090 Å. 52110 reflections collected, 6182 independent [R(int) = 0.082] used in all calculations. R_1 = 0.0306, wR_2 = 0.0775 for observed unique reflections [$I > 2\sigma(I)$] and R_1 = 0.0313, wR_2 = 0.0780 for all unique reflections. Max. and min. residual electron densities 0.48 and -1.02 e Å^{-3}. CCDC ref: 1528021.

[1^{Ph}]AlMe$_2$ and [1^{Dipp}]AlMe$_2$: The two compounds were synthesized by a common method: to a solution of [**1**^{Ph}]H/[**1**^{Dipp}]H (2.1 mmol) in toluene (25 mL) at -20^{0}C, was added a solution of $AlMe_3$ also in toluene (1.05 mL of a 2.0 M solution, 2.1 mmol) with rapid stirring. The reaction mixture was slowly warmed to room temperature and volatiles removed *in vacuo* to yield the product as a spectroscopically pure light yellow solid. Slow evaporation of a saturated toluene solution produced crystals suitable for X-ray crystallography. [**1**^{Ph}]$AlMe_2$: yield 0.98 g, 75%. ^{1}H NMR (400 MHz, C_6D_6): δ_H -0.28 ($AlCH_3$), 2.26 (s, 12H, $(CH_3)_2N$-), 4.06 (s, 1H, N-nacnac backbone CH), 6.82 (t, $^3J_{HH}$ = 7.4 Hz, 2H, *p*-CH of Ph), 6.98 (d, $^3J_{HH}$ = 7.2 Hz, 4H, *o*-CH of Ph), 7.07 (t, $^3J_{HH}$ = 7.8 Hz, 4H, *m*-CH of Ph). $^{13}C\{^1H\}$ NMR (125 MHz, C_6D_6): δ_C -8.9 ($AlCH_3$), 40.3 ($(CH_3)_2N$), 79.2 (N-nacnac backbone CH), 122.4 (*p*-CH of Ph), 125.0 (*o*-CH of Ph), 129.1 (*m*-CH of Ph), 149.1 (*ipso*-C of Ph), 166.4 (imine quaternary C). ^{27}Al NMR (104 MHz, C_6D_6): δ_{Al} 166 (br). EI-MS: (*m*/*z*, %): 349.0, 100, $[M\text{-}CH_3]^+$; 304.0, 80 $[M\text{-}2CH_3]^+$; accurate mass: calc. for $C_{20}H_{26}AlN_4$ ($[M - CH_3]^+$) 349.1967, meas. 349.0262. Elemental microanalysis: calc. for $C_{21}H_{29}AlN_4$: C 69.20, H 8.02, N 15.37%, meas. C 69.04, H 7.89, N 15.39%. Crystallographic data: $C_{21}H_{29}AlN_4$, M_r = 364.46, monoclinic, *P* 2$_1$/*c*, *a* = 25.2085(10), *b* =

9.3862(3), *c* = 18.8139(7) Å, β = 110.086(4)°, *V* = 4180.3(3) Å^3, *Z* = 8, ρ_c = 1.158 g cm^{-3}, *T* = 150 K, λ = 1.54184 Å. 30632 reflections collected, 8099 independent [R(int) = 0.109] used in all calculations. R_1 = 0.0953, wR_2 = 0.2725 for observed unique reflections [$I > 2\sigma(I)$] and R_1 = 0.1097, wR_2 = 0.2930 for all unique reflections. Max. and min. residual electron densities 0.69 and -0.65 e Å^{-3}. CCDC ref: 1528015. **[1^{Dipp}]AlMe$_2$**: yield 0.94 g, 84%. ^{1}H NMR (500 MHz, C_6D_6): δ_H -0.28 ($AlCH_3$), 1.24 (d, $^3J_{HH}$ = 6.7 Hz, 12H, (CH_3)$_2$CH), 1.40 (d, $^3J_{HH}$ = 6.7 Hz, 12H, (CH_3)$_2$CH), 2.27 (s, 12H, (CH_3)$_2$N), 3.57 (sept, $^3J_{HH}$ = 6.7 Hz, 4H, (CH_3)$_2$CH), 3.83 (s, 1H, N-nacnac backbone CH), 7.16-7.20 (6H, aromatic CH). ^{13}C{^{1}H} NMR (125 MHz, C_6D_6): δ_C -8.09 ($AlCH_3$), 24.1 ((CH_3)$_2$CH), 26.7 ((CH_3)$_2$CH), 28.4 ((CH_3)$_2$CH), 41.0 ((CH_3)$_2$N), 76.5 (N-nacnac backbone CH), 124.7 (*p*-CH of Dipp), 125.5 (*m*-CH of Dipp), 142.8 (*ipso*-C of Dipp), 144.5 (*o*-C of Dipp), 166.8 (imine quaternary C). ^{27}Al NMR (104 MHz, C_6D_6): δ_{Al} 157 (br). EI-MS: (m/z, %): 517.4, 40 [M-CH_3]$^+$; accurate mass: calc. for $C_{32}H_{50}AlN_4$ ([M–CH_3]$^+$) 517.3851, meas. 517.3889. Elemental microanalysis: calc. for $C_{33}H_{53}AlN_4$: C 74.39, H 10.03, N 10.52%, meas. C 74.59, H 10.04, N 10.44%. Crystallographic data: $C_{33}H_{53}AlN_4$, M_r = 532.79, monoclinic, *P* 2$_1$/*c*, *a* = 17.3795(3), *b* = 9.8573(1), *c* = 19.1009(3) Å, β = 101.2023(6)°, *V* = 3209.92(8) Å^3, *Z* = 4, ρ_c = 1.102 g cm^{-3}, *T* = 150 K, λ = 0.71073 Å. 13688 reflections collected, 7303 independent [R(int) = 0.042] used in all calculations. R_1 = 0.0470, wR_2 = 0.0988 for observed unique reflections [$I > 2\sigma(I)$] and R_1 = 0.0871, wR_2 = 0.1401 for all unique reflections. Max. and min. residual electron densities 0.55 and -0.52 e Å^{-3}. CCDC ref: 1528009.

[1^{Ph}]SnCl, [1^{Xyl}]SnCl and [1^{Dipp}]SnCl: The three compounds were prepared by a common method. A solution of [**1**^{R}]H (1.0 mmol, R = Ph, Xyl, Dipp) in toluene (25 mL) was treated with ^{n}BuLi (1.05 equiv.) at -78°C, and the reaction mixture warmed slowly to room temperature and stirred for 2 h. The resulting solution was added to a toluene solution (10 mL) containing $SnCl_2$ (1.05 equiv.) at -78°C, and the resulting mixture warmed to room temperature with stirring. After 12 h, volatiles were removed *in vacuo*, and the resulting residue washed with cold hexane to yield the product as near-white spectroscopically pure solid in each case. X-ray quality crystals were obtained from a solution in toluene layered with hexane and stored at -26°C. **[1^{Ph}]SnCl:** Yield 0.51 g, 69%. ^{1}H NMR (400 MHz, C_6D_6): δ_H 2.29 (s, 12H, (CH_3)$_2$N-), 4.25 (s, 1H, N-nacnac backbone CH), 6.77 (t, $^3J_{HH}$ = 7.0 Hz, 2H, *p*-CH of Ph), 6.84 (d, $^3J_{HH}$ = 8.0 Hz, 4H, *o*-CH of Ph), 7.01 (t, $^3J_{HH}$ = 7.6 Hz, 4H, *m*-CH of Ph). ^{13}C{^{1}H} NMR (100 MHz, C_6D_6): δ_C 40.6 ((CH_3)$_2$N-), 82.9 (N-nacnac backbone CH), 122.3 (*p*-CH of Ph), 123.6 (*o*-CH of Ph), 129.9 (*m*-CH of Ph), 148.9 (*ipso*-C of Ph), 165.1 (imine quaternary C). ^{119}Sn NMR (186 MHz, C_6D_6): δ_{Sn} -169 ppm. EI-MS (*m/z*, %): 462.1, 6, [M]$^+$; 426.1, 2 [M-Cl]$^+$; accurate mass: calc. for $C_{19}H_{23}ClN_4Sn$ ([M]$^+$) 462.0633, meas. 462.0678. Crystallographic data: $C_{19}H_{23}ClN_4Sn$, M_r = 461.56, triclinic, *P*-1, *a* = 8.6350(2), *b* = 9.3350(3), *c* = 13.8133(5) Å, α = 104.8910(12), β = 100.1742(12), γ = 105.6759(15), *V* = 999.15(6) Å^3, *Z* = 2, ρ_c = 1.534 g cm^{-3}, *T* = 150 K, λ = 0.71073 Å. 23131 reflections collected, 4552 independent [R(int) = 0.034] used in all calculations. R_1 = 0.0386, wR_2 = 0.0696 for observed unique reflections [$I > 2\sigma(I)$] and R_1 = 0.0561, wR_2 = 0.0878 for all unique reflections. Max. and min. residual electron densities 1.77 and -1.24 e Å^{-3}. CCDC ref: 1528017. **[1^{Xyl}]SnCl**: Yield: 0.41 g, 59%. ^{1}H NMR (400 MHz, C_6D_6): δ_H 2.02 (s, 6H, CH_3 of Xyl), 2.21 (s, 12H, (CH_3)$_2$N), 2.77 (s, 6H, CH_3 of Xyl), 4.01 (s, 1H, N-nacnac backbone CH), 7.01 – 6.84 (overlapping m, 6H, *p*- and *m*-CH of Xyl). ^{13}C{^{1}H} NMR (101 MHz, C_6D_6): δ_C 19.4, 21.9 (CH_3 of Xyl), 40.2 ((CH_3)$_2$N), 79.6 (N-nacnac backbone CH), 124.2 (*p*-CH of xyl), 129.2, 130.1 (*m*-CH of Xyl), 133.5, 133.6 (*o*-C of Xyl), 146.2 (*ipso*-C of Xyl), 165.5 (imine quaternary C). EI-MS (*m*/*z*, %): 510, 100, [M]$^+$; accurate mass: calc. for $C_{23}H_{31}ClN_4{}^{112}Sn$ 510.1285, meas. 510.1264. Crystallographic data: $C_{23}H_{31}ClN_4Sn$, M_r = 517.67, orthorhombic, *P* 2$_1$2$_1$2$_1$, *a* = 9.2745(1), *b* = 11.9112(1), *c* = 21.0381(2) Å, *V* = 2324.09(4) Å^3, *Z* = 4, ρ_c = 1.479 g cm^{-3}, *T* = 150 K, λ = 0.71073 Å. 5289 reflections collected, 5289 independent [R(int) = 0.000] used in all calculations. R_1 = 0.0218, wR_2 = 0.0468 for observed unique reflections [$I > 2\sigma(I)$] and R_1 = 0.0246, wR_2 = 0.0492 for all unique reflections. Max. and min. residual electron densities 0.53 and -0.51 e Å^{-3}. CCDC ref: 1528019. **[1^{Dipp}]SnCl**: Yield 0.52 g, 78%. ^{1}H NMR (400 MHz, C_6D_6): δ_H 1.11 (d, $^3J_{HH}$ = 6.8 Hz, 12H, (CH_3)$_2$CH-), 1.13 (d, $^3J_{HH}$ = 6.4 Hz, 12H, (CH_3)$_2$CH-), 1.28 (d, $^3J_{HH}$ = 6.4 Hz, 12H, (CH_3)$_2$CH-), 1.59 (d, $^3J_{HH}$ = 6.8 Hz, 12H, (CH_3)$_2$CH-), 2.24 (s, 12H, (CH_3)$_2$N-), 3.02 (sept, $^3J_{HH}$ = 6.7 Hz, 2H, (CH_3)$_2$CH-), 4.03 (s, 1H, N-nacnac backbone CH), 4.47 (sept, $^3J_{HH}$ = 6.7 Hz, 2H, (CH_3)$_2$CH-), 7.05-7.15 (6H, aromatic CH).^{13}C{^{1}H} NMR (100 MHz, C_6D_6): δ_C 24.0 ((CH_3)$_2$CH-), 24.2 ((CH_3)$_2$CH-), 27.0 ((CH_3)$_2$CH-), 28.3 ((CH_3)$_2$CH-), 28.3 ((CH_3)$_2$CH-), 28.4 ((CH_3)$_2$CH-), 41.3 ((CH_3)$_2$N-), 79.9 (N-nacnac backbone CH), 124.5, 125.5, 126.3, 142.1, 144.5, 145.5 (aromatic C), 165.9 (imine quaternary C). ^{119}Sn NMR (186 MHz, C_6D_6): δ_{Sn} -192 ppm. EI-MS: (*m/z*, %): 630.3, 3 [M]$^+$; 587.2, 30 [M-NMe_2]$^+$; accurate mass: calc. for $C_{31}H_{47}ClN_4{}^{116}Sn$ (M$^+$) 626.2507, meas. 626.2506. Crystallographic data: $C_{31}H_{47}ClN_4Sn$, M_r = 629.88, monoclinic, *C* 2/*c*, *a* = 34.9244(8), *b* = 9.8094(3), *c* = 19.5389(4) Å, β = 112.4405(14)°, *V* = 6186.9(3) Å^3, *Z* = 8, ρ_c = 1.352 g cm^{-3}, *T* = 150 K, λ = 0.71073 Å. 36739 reflections collected, 7035 independent [R(int) = 0.066] used in all calculations. R_1 = 0.0440, wR_2 = 0.0714 for observed unique reflections [$I > 2\sigma(I)$] and R_1 = 0.0932, wR_2 = 0.1046 for all unique reflections. Max. and min. residual electron densities 2.57 and -2.09 e Å^{-3}. CCDC ref: 1528013. CHN microanalysis measurements on the compounds [**1**^{R}]SnCl (R = Ph, Xyl, Dipp) – even those using single crystalline samples – gave reproducibly low C analysis, while giving acceptable data in each case for H and N.

[1^{Dipp}]SnH: To a toluene (30 mL) of [**1**^{Dipp}]SnCl (0.5 g, 0.8 mmol) at -78°C was added a 1.0 M solution of K[$HBEt_3$] in THF (1.05 equiv.) over a period of 5 min. The reaction mixture was warmed to room temperature and stirred for an additional 3 h before volatiles were removed *in vacuo*. The residual solid was extracted into cold hexane; storage at -26°C produced light yellow crystals suitable for X-ray crystallography. Yield: 0.066 g, 14%. ^{1}H NMR (400 MHz, C_6D_6): δ_H 1.19 (d, $^3J_{HH}$ = 6.3 Hz, 12H, (CH_3)$_2$CH-), 1.21 (d, $^3J_{HH}$ = 6.8 Hz, 12H, (CH_3)$_2$CH-), 1.27 (d, $^3J_{HH}$ = 6.8 Hz, 12H, (CH_3)$_2$CH-), 1.54 (d, $^3J_{HH}$ = 6.8 Hz, 12H, (CH_3)$_2$CH-), 2.28 (s, 12H, (CH_3)$_2$N-), 3.30 (sept, $^3J_{HH}$ = 6.8 Hz, 2H, (CH_3)$_2$CH-), 3.72 (sept, $^3J_{HH}$ = 6.7 Hz, 2H, (CH_3)$_2$CH-), 4.02 (s, 1H, N-nacnac backbone CH), 7.08-7.16 (6H, aromatic CH), 13.42 (s, 1H, SnH).^{13}C{^{1}H} NMR (100 MHz, C_6D_6): δ_C 23.9 ((CH_3)$_2$CH-), 24.1 ((CH_3)$_2$CH-), 26.7 ((CH_3)$_2$CH-), 27.8 ((CH_3)$_2$CH-), 28.3 ((CH_3)$_2$CH-), 28.4 ((CH_3)$_2$CH-), 41.5 ((CH_3)$_2$N-), 78.8 (N-nacnac backbone CH), 124.4, 124.7, 125.5, 143.8, 144.3, 145.3 (aromatic C), 167.0 (imine quaternary C). ^{119}Sn NMR (186 MHz, C_6D_6): δ_{Sn} -18 ppm. EI-MS: (m/z, %): 595.0, weak [M-H]$^+$. Crystallographic data: $C_{31}H_{48}SnN_4$, M_r = 594.43, monoclinic *P* 2$_1$/*c*, *a* = 12.4032(4), *b* = 17.2188(5), *c* = 15.4106(4) Å, β = 103.675(3)° *V* = 3197.92(17) Å^3, *Z* = 4, ρ_c = 1.235 g cm^{-3}, *T* = 150 K, λ = 1.54180 Å. 18662 reflections collected, 6621 independent [R(int) = 0.064] used in all calculations. R_1 = 0.0634, wR_2 = 0.1622 for observed unique reflections [$I > 2\sigma(I)$] and R_1 = 0.0728, wR_2 = 0.1740 for all unique reflections. Max. and min. residual electron densities 2.61 and -3.07 e Å^{-3}. CCDC ref: 1528014.

{[1^{Dipp}]Yb(μ-I)}$_2$: To a stirred solution of [**1**^{Dipp}]H (0.439 g, 0.92 mmol) in toluene (10 mL) was added KCH_2Ph (0.120 g, 0.92 mmol). A white precipitate started to form immediately and after stirring overnight at room temperature a very thick white suspension was formed. At this point, volatiles were removed *in vacuo*, and solid $YbI_2(thf)_2$ (0.527 g, 0.92 mmol) added, followed by thf (20 mL). The reaction mixture was stirred at room temperature for 12 h, producing a dark brown-red suspension. Volatiles were again removed *in vacuo,* and the residue extracted with warm benzene (3 × 10 mL). The filtrate was slowly evaporated under reduced pressure until only about 1 mL of liquid remained. The very dark brown mother liquor was decanted via a cannula and the crystalline

residue was washed with a small amount of cold benzene. Drying under vacuum yielded maroon crystals of [**1**^{Dipp}]Yb(μ-I)(THF). Yield: 0.34 g, 0.40 mmol, 43%. ^{1}H NMR (C_6D_6, 400 MHz): δ_H 0.94 (br s, 4H, CH_2 of THF), 1.38 (d, $^3J_{HH}$ = 6.7 Hz, 12H, (C<u>H</u>$_3$)$_2$CH-), 1.41 (d, $^3J_{HH}$ = 6.7 Hz, 12H, (C<u>H</u>$_3$)$_2$CH-), 2.49 (s, 12H, (C<u>H</u>$_3$)$_2$N-), 3.41 (br sept, $^3J_{HH}$ = ca. 7 Hz, 4H, (CH$_3$)$_2$C<u>H</u>-), 3.68 (br s, 4H, OCH_2 of THF), 3.80 (s, 1H, N-nacnac backbone CH), 7.02 (t, $^3J_{HH}$ = 7.6 Hz, 2H, *p*-CH of Dipp), 7.16 (m, 4H, *m*-CH of Dipp + C_6D_5H). ^{13}C{^{1}H} NMR (C_6D_6, 100 MHz): δ 162.9 (imine quaternary C), 147.5 (*ipso*-C of Dipp), 139.9 (*o*-C of Dipp), 124.3 (*m*-CH of Dipp), 122.0 (*p*-CH of Dipp), 74.2 (N-nacnac backbone CH), 69.7 (OCH_2 of THF), 40.7 ((<u>C</u>H$_3$)$_2$N-), 29.2 ((CH$_3$)$_2$<u>C</u>H-), 26.5 ((<u>C</u>H$_3$)$_2$CH-), 24.9 (CH_2 of THF), 24.0 (CH*Me*$_2$). Although single crystals of this material could not be obtained, removal of THF was possible at elevated temperatures to give samples of the donor-free dimer suitable for X-ray crystallography. A sample of [**1**^{Dipp}]Yb(μ-I)(THF) (0.149 g, 0.175 mmol) was heated slowly with a heat-gun under full vacuum. At ~80 °C the vacuum gauge showed vapour evolution, which continued over a period of 2 h with the temperature in the range of 80 to 90 °C. The originally maroon crystals turned into a red-orange material, and a small amount of [**1**^{Dipp}]H sublimed. The product was extracted with benzene (4 mL), the red-orange solution decanted from a small amount of pale precipitate and slowly evaporated at room temperature almost to dryness producing large red crystals of {[**1**^{Dipp}]Yb(μ-I)}$_2$ (suitable for crystallography) which were washed with a small amount of benzene and dried *in vacuo*. Yield: 0.105 g, 77%. ^{1}H NMR (C_6D_6, 400 MHz): δ_H 1.32 (d, $^3J_{HH}$ = 6.7 Hz, 12H, (C<u>H</u>$_3$)$_2$CH-), 1.33 (d, $^3J_{HH}$ = 6.7 Hz, 12H, (C<u>H</u>$_3$)$_2$CH-), 2.42 (s, 12H, (C<u>H</u>$_3$)$_2$N-), 3.19 (sept, $^3J_{HH}$ = 6.7 Hz, 4H, (CH$_3$)$_2$C<u>H</u>-), 3.71 (s, 1H, N-nacnac backbone CH), 6.98 (t, $^3J_{HH}$ = 7.6 Hz, 2H, *p*-CH of Dipp), 7.11 (d, $^3J_{HH}$ = 7.6 Hz, 4H, *m*-CH of Dipp). ^{13}C{^{1}H} NMR (C_6D_6, 100 MHz): δ_C 22.8 ((<u>C</u>H$_3$)$_2$CH-), 25.6 ((<u>C</u>H$_3$)$_2$CH-), 29.8 ((CH$_3$)$_2$<u>C</u>H-), 40.0 ((<u>C</u>H$_3$)$_2$N-), 71.2 (N-nacnac backbone CH), 121.8 (*p*-CH of Dipp), 124.0 (*m*-CH of Dipp), 138.7 (*o*-C of Dipp), 146.2 (*ipso*-C of Dipp), 161.8 (imine quaternary C). Elemental microanalysis: calc. for $C_{31}H_{47}N_4Yb$: C 48.00, H 6.11, N 7.22%, meas. C 47.89, H 6.04, N 7.09%. Crystallographic data: $C_{62}H_{94}I_2N_8Yb_2$ M_r = 1551.37, monoclinic, *P* 2$_1$/*n*, *a* = 20.2293(6), *b* = 17.2389(4), *c* = 20.7063(6) Å, β = 114.666(4)°, *V* = 6562.1(4) Å^3, *Z* = 4, ρ_c = 1.570 g cm^{-3}, *T* = 150 K, λ = 1.54180 Å. 39921 reflections collected, 13613 independent [R(int) = 0.043] used in all calculations. R_1 = 0.0419, wR_2 = 0.0994 for observed unique reflections [$I > 2\sigma(I)$] and R_1 = 0.0531, wR_2 = 0.1082 for all unique reflections. Max. and min. residual electron densities 3.12 and -2.44 e Å^{-3}. CCDC ref: 1528007.

[1^{Dipp}]$_2$Yb: To a mixture of [**1**^{Dipp}]K (prepared *in situ* from [**1**^{Dipp}]H (0.104 g, 0.22 mmol) and KCH_2Ph (0.029 g, 0.22 mmol) in toluene and dried *in vacuo*) and [**1**^{Dipp}]Yb(μ-I)(THF) (0.185 g, 0.22 mmol) was added THF (ca. 5 mL) by vacuum transfer. The mixture was warmed to 55 °C and agitated by hand until a dark brown suspension was formed. At this point, volatiles were removed *in vacuo*, and the residue extracted with benzene (2 mL) and transferred into a crystallisation tube. After drying *in vacuo*, hexane (ca. 2 mL) was vacuum transferred into the tube, which was then sealed. After gentle warming, the resulting dark brown solution was decanted from the accompanying grey precipitate into the second part of the tube, concentrated (to form viscous oil) and stored in a freezer at −30°C for 2 d. This led to the formation of colourless crystals of [**1**^{Dipp}]H and nearly black crystals of [**1**^{Dipp}]$_2$Yb, which were washed with hexane (once crystallised it was poorly soluble in this solvent) and dried *in vacuo*. Yield: 0.095 g, 0.084 mmol, 38%. ^{1}H NMR (C_6D_6, 400 MHz): δ_H 0.42 (d, $^3J_{HH}$ = 6.7 Hz, 3H, (C<u>H</u>$_3$)$_2$CH-), 0.60 (d, $^3J_{HH}$ = 6.7 Hz, 3H, (C<u>H</u>$_3$)$_2$CH-), 1.02 (d, $^3J_{HH}$ = 6.7 Hz, 3H, (C<u>H</u>$_3$)$_2$CH-), 1.05 (d, $^3J_{HH}$ = 6.7 Hz, 3H, (C<u>H</u>$_3$)$_2$CH-), 1.17 (m, 15H, (C<u>H</u>$_3$)$_2$CH-), 1.20 (d, $^3J_{HH}$ = 6.7 Hz, 3H, (C<u>H</u>$_3$)$_2$CH-), 1.23 (d, $^3J_{HH}$ = 6.7 Hz, 3H, (C<u>H</u>$_3$)$_2$CH-), 1.29 (d, $^3J_{HH}$ = 6.7 Hz, 3H, (C<u>H</u>$_3$)$_2$CH-), 1.35 (d, $^3J_{HH}$ = 6.7 Hz, 3H, (C<u>H</u>$_3$)$_2$CH-), 1.42 (d, $^3J_{HH}$ = 6.7 Hz, 3H, (C<u>H</u>$_3$)$_2$CH-), 1.47 (d, $^3J_{HH}$ = 6.7 Hz, 3H, (C<u>H</u>$_3$)$_2$CH-), 1.53 (d, $^3J_{HH}$ = 6.7 Hz, 3H, (C<u>H</u>$_3$)$_2$CH-), 2.24 (br s, 3H, (C<u>H</u>$_3$)$_2$N-), 2.35 (s, 3H, (C<u>H</u>$_3$)$_2$N-), 2.40 (two s, 12H, (C<u>H</u>$_3$)$_2$N-), 2.83 (br s, 3H, (C<u>H</u>$_3$)$_2$N-), 2.85-3.02 (overlapping septets, 4H, (CH$_3$)$_2$C<u>H</u>-), 3.06 (sept, $^3J_{HH}$ = 6.7 Hz, 1H, (CH$_3$)$_2$C<u>H</u>-), 3.11 (br s, 3H, (C<u>H</u>$_3$)$_2$N-), 3.24 (sept, $^3J_{HH}$ = 6.7 Hz, 1H, (CH$_3$)$_2$C<u>H</u>-), 3.26 (s, 1H, N-nacnac backbone CH), 3.37 (sept, $^3J_{HH}$ = 6.7 Hz, 1H, (CH$_3$)$_2$C<u>H</u>-), 3.64 (sept, $^3J_{HH}$ = 6.7 Hz, 1H, (CH$_3$)$_2$C<u>H</u>-), 6.75 (d, $^3J_{HH}$ = 7.6 Hz, 1H, *m*-CH of Dipp), 6.86 (t, $^3J_{HH}$ = 7.6 Hz, 1H, *p*-CH of Dipp), 6.90-7.19 (m, 8H, CH of Dipp), 7.32 (d, $^3J_{HH}$ = 7.6 Hz, 1H, *m*-CH of Dipp), 7.36 (d, $^3J_{HH}$ = 7.6 Hz, 1H, *m*-CH of Dipp). ^{13}C{^{1}H} NMR (C_6D_6, 100 MHz): δ_C 21.5, 22.2, 22.4, 23.6, 24.1, 24.3, 24.4, 24.4, 24.5, 24.8, 25.9, 26.1, 26.2, 27.5 ((<u>C</u>H$_3$)$_2$CH-), 27.3, 28.3, 28.5, 28.6, 29.0, 29.3, 30.0, 30.2 ((CH$_3$)$_2$<u>C</u>H-), 39.8, 40.4, 40.7, 41.3, 41.8, 43.0 ((<u>C</u>H$_3$)$_2$N-), 66.2, 67.2 (N-nacnac backbone CH), 121.3, 121.5, 121.8, 122.4, 122.5, 123.6, 123.6, 123.8, 124.3, 124.5, 124.8, 125.2 (CH of Dipp); 137.6, 139.0, 139.2, 139.3, 139.5, 139.8, 134.0, 140.1 (*o*-C of Dipp); 146.1, 147.4, 148.0 (*ipso*-C of Dipp); 161.9, 162.9, 163.2 (imine quaternary C). A sample of [**1**^{Dipp}]$_2$Yb for X-ray crystallography was prepared from [**1**^{Dipp}]K (0.051 g, 0.099 mmol) and $YbI_2(thf)_2$ (0.020 g, 0.035 mmol) using a similar procedure. Crystallographic data: $C_{62}H_{94}N_8Yb$, M_r = 1124.52, orthorhombic, *P* 2$_1$2$_1$2$_1$, *a* = 14.3829(1), *b* = 15.0030(1), *c* = 27.5152(2) Å, *V* = 5937.41(7) Å^3, *Z* = 4, ρ_c = 1.258 g cm^{-3}, *T* = 150 K, λ = 1.54180 Å. 70955 reflections collected, 12348 independent [R(int) = 0.025] used in all calculations. R_1 = 0.0167, wR_2 = 0.0431 for observed unique reflections [$I > 2\sigma(I)$] and R_1 = 0.0173, wR_2 = 0.0434 for all unique reflections. Max. and min. residual electron densities 0.30 and -0.43 e Å^{-3}. CCDC ref: 1528008.

Crystallography

Diffraction data were collected using a Nonius Kappa CCD or Oxford Diffraction (Agilent) SuperNova diffractometer at 150 K; data were reduced using either DENZO, SCALEPACK or CrysAlisPro, and the structures were solved with either SIR92, SuperFlip or SHELXT and refined with full-matrix least squares within CRYSTALS or SHELXL-2014, as described in the CIF.[21] Complete details of the X-ray analyses have been deposited at The Cambridge Crystallographic Data Centre (CCDC 1528007-1528025).

Computational Method

Geometry optimization were performed using the Amsterdam Density Functional (ADF) 2014 software package. Calculations were performed using the Vosko-Wilk-Nusair local density approximation with exchange from Becke, and correlation correction from Perdew, and 3-dimension dispersion effect (BP86-D3).[22] Slater-type orbitals (STOs) were used for the triple zeta basis set with an additional set of polarization functions (TZP). The full-electron basis set approximation was applied with no molecular symmetry. General numerical quality was good. Run files for each of the calculations are included in the SI.

Acknowledgements

We acknowledge funding from the Jardine Foundation (DCHD), the EPSRC (AP, grant number EP/L025000/1), EU Marie Curie program (ELK, grant number PIEF-GA-2013-626441) and the ARC (CJ, AS, SA). We also thanks Drs Jesus Campos and Rémi Tirfoin for additional crystallography, and Reike Clauss for additional synthetic work.

[1] For early references, see: a) W. Bradley, I. Wright, *J. Chem. Soc.* **1956**, 640-648; b) J. E. Parks, R. H. Holm, *Inorg. Chem.* **1968**, *7*, 1408–1416; c) S. G. McGeachin, *Can. J. Chem.* **1968**, *46*, 1903–1912; d) C. L.

Honeybourne, G. A. Webb, *Chem. Commun. (London)* **1968**, 739-740; e) R. Bonnett, D. C. Bradley, K. J. Fisher, *Chem. Commun*. **1968**, 886-887.

[2] L. Bourget-Merle, M. F. Lappert, J. R. Severn, *Chem. Rev.* **2002**, *102*, 3031-3066.

[3] See, for example: a) M. S .Hill, P. B. Hitchcock, R. Pongtavornpinyo, *Science* **2006**, *311*, 1904-1907; b) S. P. Green, C. Jones, A. Stasch, *Science* **2007**, 318, 1754-1757; c) M. M. Rodriguez, E. Bill, W. W. Brenessel, P. L Holland, *Science* **2011**, *334*, 780-783.

[4] For selected recent reviews encompassing aspects of Nacnac chemistry, see: a) M. Asay, C. Jones, M. Driess, *Chem. Rev.* **2011**, *111*, 354-396; b) Y. Tsai, *Coord. Chem. Rev*. **2012**, *256*, 722; c) C. Chen, S. M. Bellows, P. L. Holland, *Dalton Trans.* **2015**, *44*, 16654-16670; d) C. Camp, J. Arnold, *Dalton Trans.* **2016**, *45*, 14462-14498.

[5] See, for example: a) D. T. Carey, E. K. Cope-Eatough, E. Vilapana-Mafé, F. S. Mair, R. G. Pritchard, J. E. Warren, R. J. Woods, *Dalton Trans.* **2003**, 1083-1093; b) Y. Cheng, D. J. Doyle, P. B. Hitchcock, M. F. Lappert; *Dalton Trans.* **2006**, 4449-4460; c) M. P. Romero-Fernández, M. Ávalos, R. Babiano, P. Cintas, J. L. Jiménez, M. E. Light, J. C. Palacios, *Org. Biomol. Chem.* **2014**, *12*, 8997-9010. C_6F_5 groups have also been employed as electron-withdrawing N-aryl groups: D. Vidovic, J. N. Jones, J. A. Moore, A. H. Cowley, *Z. Anorg. Allg. Chem.* **2005**, *631*, 2888-2892.

[6] C. Jones, *Coord. Chem. Rev.* **2010**, *254*, 1273-1289.

[7] P. T. K. Lee, Masters Thesis, St. Mary's University, Halifax, Canada, 2009.

[8] a) Z. Janousek, H. G. Viehe, *Angew. Chem., Int. Ed. Engl.* **1971**, *10*, 574-575; b) S. Brenner, H. G. Viehe, *Tetrahedron Lett.* **1976**, *17*, 1617-1620.

[9] See also: a) A. Albers, T. Bayer, S. Demeshko, S. Dechert, F. Meyer, *Chem.-Eur. J.* **2013**, *19*, 10101-10106. For a very recent example of a cationic carbene featuring a related backbone, see: b) V. Regnier, Y. Planet, C.E. Moore, J. Pecaut, C. Philouze, D. Martin, *Angew. Chem. Int. Ed.* **2017**, *56*, 1031-1035.

[10] M. Stender, R. J. Wright, B. E. Eichler, J. Prust, M. M. Olmstead, H. W. Roesky, P. P. Power, *Dalton Trans.* **2001**, 3465-3469.

[11] J. Emsley in *The Elements* 3rd edition, Clarendon Press, Oxford, **1998**.

[12] J. Feldman, S. J. McLain, A. Parthasarathy, W. J. Marshall, J. C. Calabrese, S. D Arthur, *Organometallics* **1997**, *16*, 1514.

[13] a) A. Akkari, J. J. Byrne, I Saur, G. Rima, H. Gornitzka, J. Barrau, *J. Organomet. Chem.* **2001**, *622*, 190-198; b) A. E. Ayers, T. M. Klapötke, H. V. R. Dias, *Inorg. Chem.* **2001**, *40*, 1000-1005; c) Y. Ding, H. W. Roesky, M. Noltemeyer, H.-G. Schmidt, P. P. Power, *Organometallics* **2001**, *20*, 1190-1194; d) L. W. Pineda, V. Jancik, K. Starke, R. B. Oswald, H. W. Roesky, *Angew. Chem., Int. Ed.* **2006**, *45*, 2602-2605.

[14] a) S. Harder, *Angew. Chem. Int. Ed.* **2004**, *43*, 2714-2718; b) P.B. Hitchcock, A. V. Khvostov, M. F. Lappert, A. V. Protchenko, *Dalton Trans*. **2009**, 2383-2391.

[15] For a related lithium Nacnac derivative see: a) C. Cui, H. W. Roesky, H. Hao, H.-G. Schmidt, M. Noltemeyer, *Angew. Chem., Int. Ed.* **2000**, *39*, 1815. Binuclear systems have been reported in association with aryl groups bearing donor substituents: b) J. Liu, L. Vieille-Petit, A. Linden, X. Luan, R. Dorta *J. Organomet. Chem.* **2012**, *719*, 80-86.

[16] For related magnesium Nacnac derivatives see reference 3b.

[17] For related aluminium Nacnac derivatives, see: a) B. Qian, D. L. Ward, M. R. Smith III, *Organometallics* **1998**, *17*, 3070-3076; b) C. E. Radzewich, M. P. Coles, R. F. Jordan, *J. Am. Chem. Soc.* **1998**, *120*, 9384-9385.

[18] E. Pretsch, P. Bühlmann, M. Badertscher in *Structure Determination of Organic Compounds* (eds. M. Badertscher, P. Bühlmann, E. Pretsch), Springer-Verlag, Berlin, 2009, Chp. 5.

[19] See also: W. E. Piers, *Coord. Chem. Rev.* **2002**, *233-234*, 131-155.

[20] For early examples of *f*-element Nacnac chemistry see: a) P. B. Hitchcock, S. A. Holmes, M. F. Lappert, S. Tian, *J. Chem. Soc., Chem. Commun.* **1994**, 2691-2692; b) D. Drees, J. Magull, *Z. Anorg. Allg. Chem.* **1994**, *620*, 814-818.

[21] a) J. Cosier, A.M. Glazer, *J. Appl. Crystallogr.* **1986**, *19*, 105-107; b) Z. Otwinowski, W. Minor, in *Methods Enzymol., Vol 276*: *Macromolecular Crystallography*, *Part A* (Eds.: C.W. Carter, Jr., R.M. Sweet) Academic Press, New York, **1997**, pp. 307-326; c) A. Altomare, G. Cascarano, C. Giacovazzo, A. Guagliardi, *J. Appl. Crystallogr.* **1994**, *27*, 1045-1050; d) L. Palatinus, G. Chapuis, *J. Appl. Crystallogr.* **2007**, *40*, 786-790; e) P.W. Betteridge, J.R. Carruthers, R.I. Cooper, K. Prout, D.J. Watkin, *J. Appl. Crystallogr.* **2003**, *36*, 1487; f) R.I. Cooper, A.L. Thompson, D.J. Watkin, *J. Appl. Crystallogr.* **2010**, *43*, 1100-1107; g) A.L. Thompson, D. J. Watkin, *J. Appl. Crystallogr.* **2011**, *44*, 1017-1022.

[22] a) A. D. Becke, *Phys. Rev. A* **1988**, *38*, 3098-3100; b) J. P. Perdew, *Phys. Rev. B* **1986**, *33*, 8822-8824; c) J. G. Snijders, P. Vernooijs, E. J. Baerends, *Atomic Data and Nuclear Data Tables*, **1982**, *26*, 483-509.

10.1002/chem.201700757

WILEY-VCH

Entry for the Table of Contents (Please choose one layout)

Layout 1:

FULL PAPER

N-nacnac-ed

The synthesis and coordination chemistry of electron-rich amino-functionalized β-diketiminato (N-nacnac) ligands are reported. Two synthetic methodologies have been developed for protio-ligands bearing backbone NR_2 groups, which react with metal alkyls to access complexes from groups 1, 2 and 13. Sn^{II} and Yb^{II} systems can be prepared via trans-metallation to allow direct comparison with conventional Nacnac compounds.

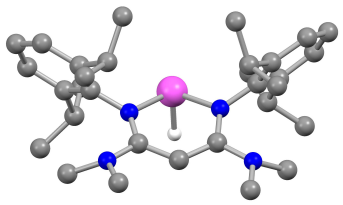

Dinh Cao Huan Do, Ailsa Keyser, Andrey V. Protchenko, Brant Maitland, Indrek Pernik, Haoyu Niu, Eugene L. Kolychev, Arnab Rit, Dragoslav Vidovic, Andreas Stasch, Cameron Jones,* and Simon Aldridge**

Page No. – Page No.

Highly electron rich β-diketiminato systems: Synthesis and coordination chemistry of amino functionalized 'N-nacnac' ligands